Rhodium-Catalyzed Asymmetric Dehydrocoupling-Cyclophosphination of Supermesitylphosphines. Enantioselective Synthesis of a P-Stereogenic Benzophospholane via C-H Activation-Functionalization

Sarah T. Chachula,[a] Russell P. Hughes,[a]* and David S. Glueck [a]*

[a] 6128 Burke Laboratory, Department of Chemistry, Dartmouth College, Hanover, New Hampshire 03755, United States

ABSTRACT: M(diphos*) catalyst precursors (M = Co or Rh) converted supermesitylphosphines PHR(Mes*) to cyclophosphinated P(2,4-(*t*-Bu)$_2$C$_6$H$_2$(6-CMe$_2$CH$_2$))(R) (R = H, Me, Ph) slowly at room temperature (Mes* = 2,4,6-(*t*-Bu)$_3$C$_6$H$_2$). Dehydrocoupling-cyclophosphination of PHPh(Mes*) occurred in up to 85:15 enantiomeric ratio (er) with [Rh((*R,R*)-Me-DuPhos)(Cl)]$_2$ and NaOSiMe$_3$. Diastereoselective formation of the resting state Rh-hydrides Rh(diphos*)(P(2,4-(*t*-Bu)$_2$C$_6$H$_2$(6-CMe$_2$CH$_2$))(R))(H) (**10**-**12**) suggested that substitution of the phosphine product by substrate was rate-determining, consistent with faster turnover for smaller ligands, with the lowest bite angles. We propose that P-H oxidative addition in Rh(diphos*)(PHR(Mes*))(H) (**15**) gave Rh(diphos*)(PR(Mes*))(H)$_2$ (**16**), whose reductive elimination of H$_2$ formed Rh(diphos*)(PR(Mes*)) (**13**), in which C-H oxidative addition of an *o*-*t*-Bu methyl group followed by P-C reductive elimination gave the resting state. Density functional theory (DFT) studies suggested that both P-H oxidative addition of PH(Ph)(Mes*) and P-C reductive elimination from Rh-PPh(Mes*) groups proceeded with inversion of configuration at three-coordinate phosphorus, and enantioselection occurred due to rapid interconversion of Rh-phosphido diastereomers **13** (R = Ph) by pyramidal inversion, along with their relative speciation and C-H activation rates. Intrinsic Bond Orbital (IBO) analyses of the P-H and C-H activation steps are consistent with proton, rather than hydride, transfer to the metal, which may be more widely relevant in such processes.

INTRODUCTION

Chiral phospholanes in the BPE and DuPhos families are privileged ligands in asymmetric catalysis,[1] and P-stereogenic analogues such as TangPhos are also highly effective (Chart 1).[2] Annulation in P-stereogenic benzophospholanes increases ligand rigidity and, in some cases, air-stability in DuanPhos,[3] BeePhos,[4] MeO-BIBOP,[5] and related derivatives. To prepare such high-value targets and to increase their structural diversity, several synthetic methods have been investigated, including resolution, use of chiral auxiliaries, and asymmetric catalysis.[6]

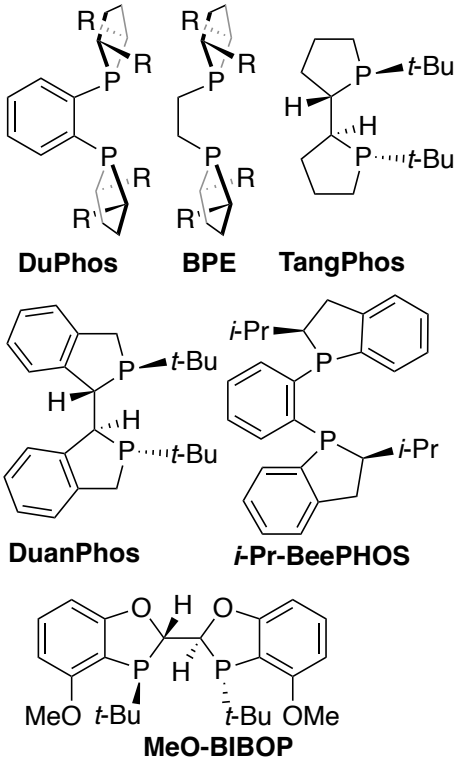

Chart 1. Selected Chiral Phospholanes, Including P-Stereogenic Benzophospholanes

Another possible route to a specific class of P-stereogenic benzophospholanes exploits C-H activation of an *ortho t*-Bu group in the bulky supermesityl (Mes* = 2,4,6-(t-Bu)$_3$C$_6$H$_2$) substituent, as in the Rh-catalyzed dehydrocoupling-cyclophosphination in Scheme 1.[7] This type of cyclization has been known since 1983, when Yoshifuji showed that heating Mes*PCl$_2$ in the presence of pyridine gave the chlorobenzophospholane P(2,4-(t-Bu)$_2$C$_6$H$_2$(6-CMe$_2$CH$_2$))(Cl).[8] Similar processes are common in low-coordinate Mes*P derivatives, also occurring upon generation of the phosphinidene intermediate[9] Mes*P or the phosphenium ions [Mes*PR]$^+$,[10] or in metal-mediated reactions.[11] The resulting bulky, rigid, P-stereogenic benzophospholanes are potentially useful ligands,[12] but stereocontrolled syntheses have not yet been reported.

Scheme 1. Proposed Mechanisms[7] of Rhodium-Catalyzed Dehydrocoupling-Cyclophosphination of PH$_2$Mes* ([Rh] = Rh(dippe))

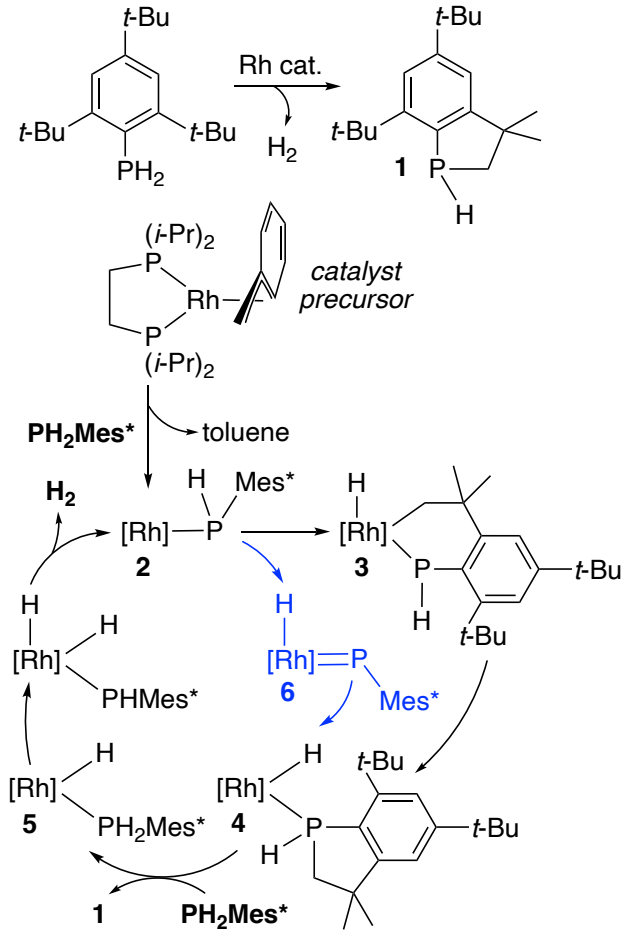

To develop such processes, we considered the proposed mechanism in Scheme 1, in which treatment of the catalyst precursor[13] Rh(dippe)(η^3-CH$_2$Ph) with PH$_2$Mes* yields toluene and the three-coordinate Rh(I)-phosphido complex Rh(dippe)(PHMes*) (**2**, dippe = (i-Pr)$_2$PCH$_2$CH$_2$P(i-Pr)$_2$)), which can undergo two possible reactions.[7] In one, C-H activation of a Mes* *ortho t*-butyl group yields the five-coordinate cyclometalated Rh(III) hydride **3**. P-C reductive elimination then gives square planar Rh(I) hydride **4**, which was observed as the catalytic resting state. After ligand substitution of secondary phosphine **1** by the primary phosphine substrate, P-H oxidative addition in **5**, followed by reductive elimination of H$_2$, would regenerate phosphido complex **2**. Alternatively, P-H α-elimination in **2** could yield phosphinidene hydride complex **6**,[14] in which P-mediated C-H activation would yield resting state **4**. These pathways could not be distinguished by labelling studies with PD$_2$Mes* because of rapid D exchange into the P-*i*-Pr groups.[7]

We hypothesized that replacing the primary phosphine PH$_2$Mes* with a secondary phosphine PHR(Mes*) would provide more mechanistic information, since α-elimination in a Rh-PR(Mes*) intermediate would be unlikely. If this step was required in catalysis, then secondary phosphines would not react. Further, replacing dippe with a chiral bis(phosphine) diphos* might enable enantioselective catalysis, because the two diastereomers of the phosphido complex Rh(diphos*)(PR(Mes*)), an analogue of **2**, might be formed selectively and/or react at different rates.[15]

We report here that investigating these ideas resulted in the development of a new catalytic asymmetric synthesis of a P-stereogenic benzophospholane and evidence for Rh-centered C-H activation in these processes. Density functional theory (DFT) studies provided more information on the stereochemistry of the fundamental steps and the origin of enantioselectivity.

RESULTS AND DISCUSSION

Rhodium- or Cobalt-Catalyzed Dehydrocoupling-Cyclophosphination Was Slow at Room Temperature and Occurred in Up to 85:15 Enantiomeric Ratio (er) Dehydrocoupling-cyclophosphination of the supermesitylphosphines PHR(Mes*) (R = H, Me, Ph) was catalyzed by the precursors Rh(diphos*)(η^3-CH$_2$Ph), a combination of [Rh(diphos*)(Cl)]$_2$ and NaOSiMe$_3$,[16] or Co(diphos*)Cl$_2$ and NaBHEt$_3$, which presumably generates [Co(diphos*)(H)]$_2$ (Scheme 2 and Table 1).[17] With 10-20 mol % catalyst loading in THF at room temperature, these reactions were very slow, taking days or weeks and frequently not reaching full conversion, although formation of byproducts was not observed and the active catalysts often remained intact (see below for details). The known products **1** and **7** were identified by ^{31}P{^{1}H} NMR spectroscopy.[18] The new phenylphosphine **8** was prepared independently and converted to its oxide **9** for assay of its enantiopurity with the chiral amino acid *S*-FmocTrp(Boc)-OH (Scheme 3).[19]

Scheme 2. Rhodium- or Cobalt-Catalyzed Dehydrocoupling-Cyclophosphination of Supermesitylphosphines

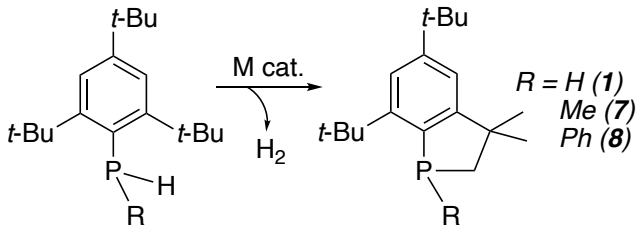

Table 1. Catalytic Dehydrocoupling-Cyclophosphination of PHR(Mes*)[a]

Entry	R	Precursor/Loading (mol %)	Time	Conversion (%)	er
1	H	Rh((*R*,*R*)-*i*-Pr-DuPhos)(CH_2Ph) (10)	5 d	100	1:1
2	H	Rh((*R*,*R*)-*i*-Pr-DuPhos)(CH_2Ph)/$NaOSiMe_3$ (10)	2 weeks	100	1:1
3	H	Co((*R*,*R*)-*i*-Pr-DuPhos)Cl_2/$NaBHEt_3$ (11)	20 h	100	1:1
4	H	Rh(dppf)(CH_2Ph) (20)	2 weeks	100	1:1
5	Ph	[Rh((*R*,*R*)-*i*-Pr-DuPhos)Cl]$_2$/$NaOSiMe_3$ (20)	3 d, 60 °C	95	nd
6	Ph	[Rh((*R*,*R*)-*i*-Pr-DuPhos)(Cl)]$_2$/$NaOSiMe_3$ (20)	6 weeks	74	25:75
7 [b]	Ph	[Rh((*R*,*R*)-Me-DuPhos)(Cl)]$_2$/$NaOSiMe_3$ (20)	3 d	100 (63% yield)	85:15
8	Ph	[Rh((*R*,*R*)-Me-DuPhos)(Cl)]$_2$/$NaOSiMe_3$ (20)	2 h, 55 °C	100	81:19[c]
9	Ph	[Rh((*R*,*R*)-Me-FerroLANE)(Cl)]$_2$/$NaOSiMe_3$ (20)	5 weeks	70	86:14
10	Ph	[Rh(*R*,*R*)-Ph-BPE)(Cl)]$_2$/$NaOSiMe_3$ (20)	6 weeks	75	42:58
11	Ph	[Rh((*S*)-BINAP)(Cl)]$_2$/$NaOSiMe_3$ (20)	6 weeks	74	61:39
12	Ph	[Rh(dppf)(Cl)]$_2$/$NaOSiMe_3$ (20)	5 weeks	92	1:1
13	Ph	Co((*R*,*R*)-*i*-Pr-DuPhos)Cl_2/$NaBHEt_3$ (9)	4 d	25	nd
14	Ph	Co((*R*,*R*)-Me-DuPhos)Cl_2/$NaBHEt_3$ (25)	3 weeks	0	nd
15	Me	[Rh((*R*,*R*)-*i*-Pr-DuPhos)Cl]$_2$/$NaOSiMe_3$ (20)	7 d	11	nd
16	Me	[Rh((*R*,*R*)-Me-DuPhos)Cl]$_2$/$NaOSiMe_3$ (17)	7 d	10	nd
17	Me	Co((*R*,*R*)-*i*-Pr-DuPhos)Cl_2/$NaBHEt_3$ (27)	4 d	0	nd
18	Me	Co((*R*,*R*)-Me-DuPhos)Cl_2/$NaBHEt_3$ (14)	3 weeks	trace	nd

[a] See the experimental section for general procedures, and the SI for details. Catalytic reactions were carried out in THF at room temperature, except for entries 5 and 8. Catalyst loading ranged from 9 to 27 mol %, and the amount of substrate from 0.1 to 0.3 mmol; nd = not determined. Conversion and product er were determined by $^{31}P\{^1H\}$ NMR spectroscopy, for which peak overlap increased the uncertainty in the er values (see the SI). For example, the reported er of 85:15, as in entry 7, could range from 90:10 to 80:20. [b] In a duplicate experiment, the reaction was not monitored until day 8, when 100% conversion had occurred. After workup, the phosphine oxide **9** was isolated in 63% yield and 85:15 er. [c] Increased $^{31}P\{^1H\}$ NMR peak overlap for this assay increased the uncertainty in the er determination, with er values estimated to range from 90:10 to 70:30.

Scheme 3. Independent Synthesis of Phenylphosphine **8** and Conversion to Its Oxide **9**, with the Chiral Amino Acid Used for $^{31}P\{^1H\}$ NMR Analysis of Enantiomeric Enrichment

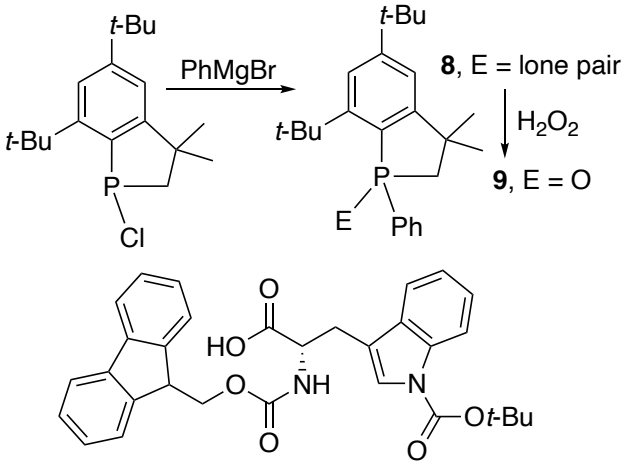

As observed with the Rh(dippe) catalyst in Scheme 1, Rh(*i*-Pr-DuPhos)-catalyzed reaction of PH_2Mes^* was slow at room temperature (Table 1, entries 1-2). The analogous cobalt catalyst was much faster (entry 3), but secondary phosphine **1** was formed without enantioselectivity with either metal, as shown by complexation to a chiral Pd-amine complex (see the SI for details, including comparison to results with the achiral Rh(dppf) catalyst (entry 4)).[20] This was not surprising, because the P-epimerization of P-stereogenic secondary phosphines catalyzed by trace acids has frustrated most previous attempts at their asymmetric synthesis.[21] Attempted removal of acid by carrying out the catalytic reaction in the presence of added $NaOSiMe_3$ (Table 1, entry 2) did not provide any improvement.[22]

With the diarylphosphine PHPh(Mes*), catalytic reactions were extremely slow at room temperature and showed marked ligand effects (Table 1, entries 5-14). With 20 mol % of the precursors [Rh(diphos*)(Cl)]$_2$ and $NaOSiMe_3$, the Me-DuPhos catalyst, for which the reaction was complete in 3 d, was much faster than the *i*-Pr-DuPhos one, which led to only 74% conversion even after 6 weeks (entries 6-7). Other Rh catalysts bearing ligands with a variety of P-

donors and bite angles were also very slow (entries 9-12), although mild heating (entries 5 and 8) greatly increased the rate. Analogous cobalt precursors were slow or ineffective (entries 13-14).

With PHPh(Mes*) and the most active Rh(Me-DuPhos) catalyst, treatment of reaction mixtures with H_2O_2 enabled isolation of phosphine oxide **9** by chromatography on silica in 63% yield (entry 7). After addition of the chiral amino acid *S*-Fmoc-Trp(Boc)-OH (Scheme 3), the $^{31}P\{^1H\}$ NMR spectrum showed two overlapping signals near 55 ppm (THF). Integration gave the enantiomeric ratio (er) of the phosphine oxide **9** and thereby the enantioselectivity in Rh-catalyzed formation of phosphine **8**. Similarly, with incomplete conversion by other catalysts (entries 6 and 9-12), the same assay without isolation of **9** gave the er values in Table 1. Dehydrocoupling-cyclophosphination was enantioselective with all the chiral Rh catalysts, with product ratios ranging from 42:58 with (*R,R*)-Ph-BPE (entry 10) to 85:15 with (*R,R*)-Me-DuPhos or (*R,R*)-Me-FerroLANE (entries 6 and 9). Peak overlap in the $^{31}P\{^1H\}$ NMR spectra of the phosphine oxide/amino acid mixture reduced the accuracy of the er values, with some variation in individual spectra, so that the reported 85:15 ratio, for example, could span a range from 90:10 to 80:20. These assay limitations made quantitative comparison difficult, but heating the catalytic reaction appeared to reduce the enantioselectivity (compare entries 7 and 8).

Rh-catalyzed reactions of the alkyl(arylphosphine) PHMe(Mes*) were much slower than for PHPh(Mes*), despite its smaller size, and cobalt catalysts were ineffective (Table 1, entries 15-18).

Observation of The Resting State Hydride Complexes Rh(diphos*)(P(2,4-(*t*-Bu)$_2$C$_6$H$_2$(6-CMe$_2$CH$_2$))(R))(H) (10-12) Suggested a Mechanism for Catalysis Involving Oxidative Addition and Reductive Elimination Steps

Although the catalytic reactions were very slow at room temperature, the mixtures were robust. Catalytic turnover continued for weeks, and the phosphine hydride intermediates **10**-**12**, analogues of **4** (Scheme 1), were observed as resting states by $^{31}P\{^1H\}$ NMR spectroscopy (Scheme 4 and Table S2 in the Supporting Information). In some cases, signals due to the two diastereomers were observed, with selectivity ranging from 2:1 for Rh((*R,R*)-*i*-Pr-DuPhos)(**1**)(H) to 10:1 for Rh((*R,R*)-*i*-Pr-DuPhos)(**8**)(H). $^{31}P\{^1H\}$ NMR data were similar to those for Rh(dippe) complex **4** and for the related hydride complex Rh((*R,R*)-*i*-Pr-DuPhos)(PPh$_3$)(H).[16b] Rhodium hydride ^1H NMR signals, which also resembled those of known analogues, were also observed in some cases (Table S2), but were not investigated for all catalysts.

Scheme 4. The Resting State Hydride Complexes **10**-**12** Were Observed by $^{31}P\{^1H\}$ NMR Spectroscopy During Rh-Catalyzed Dehydrocoupling-Cyclophosphination

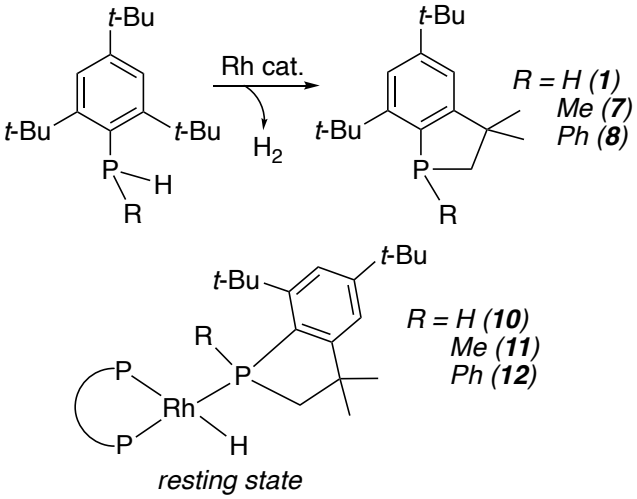

These observations are consistent with the C-H activation mechanism proposed for the Rh(dippe) catalyst and suggest that a Rh-phosphinidene mechanism is less likely, at least for secondary phosphine substrates yielding products **7**-**8**. Therefore, we propose the catalytic mechanism of Scheme 5, which shows two pathways in which the diastereomeric intermediates differ only in the P-configuration of the PMes* groups. Please also see the next section and Figure 1 for computational studies of this mechanism and lettered model intermediates **A**-**P** in Scheme 5.

The key three-coordinate Rh(diphos*)(PR(Mes*)) (**13**-**13'**) could be formed with loss of toluene from Rh-benzyl precursors and the starting phosphine, or via proton transfer from a Rh-silanolate complex, as in related chemistry with other metals.[23] After C-H activation to yield Rh(III) hydrides **14**-**14'**, P-C reductive elimination yields the resting state Rh(I) hydrides **10**-**12** and **10'**-**12'**. After ligand substitution with the substrate to give unobserved Rh(diphos*)(PHR(Mes*))(H) (**15**-**15'**), P-H oxidative addition gives **16**-**16'** and reductive elimination of H_2 regenerates the intermediates **13**-**13'**. The observation of resting states **10**-**12** and **10'**-**12'** and the steric and bite angle effects suggest that the rate-determining step is ligand substitution, which is presumably associative, as in other square planar d^8 complexes.[24] Steric hindrance to coordination of two bulky Mes*-phosphines to Rh would slow this step and account for the slow catalytic turnover.

Scheme 5. Proposed Mechanism of Rh-Catalyzed Asymmetric Dehydrocoupling-Cyclophosphination (*[Rh] = Rh(diphos*)) via Two Diastereomeric Pathways (Red and Blue), Highlighting the Selectivity-Controlling P-Inversion, Oxidative Addition, and P-C Reductive Elimination Steps. The Letters **A**-**P** Correspond to Computational Models For the Proposed Intermediates With Diphos* = (*R,R*)-Me-DuPhos, R = Ph, and the Mes* *p*-*t*-Bu Group Omitted (Figure 1)

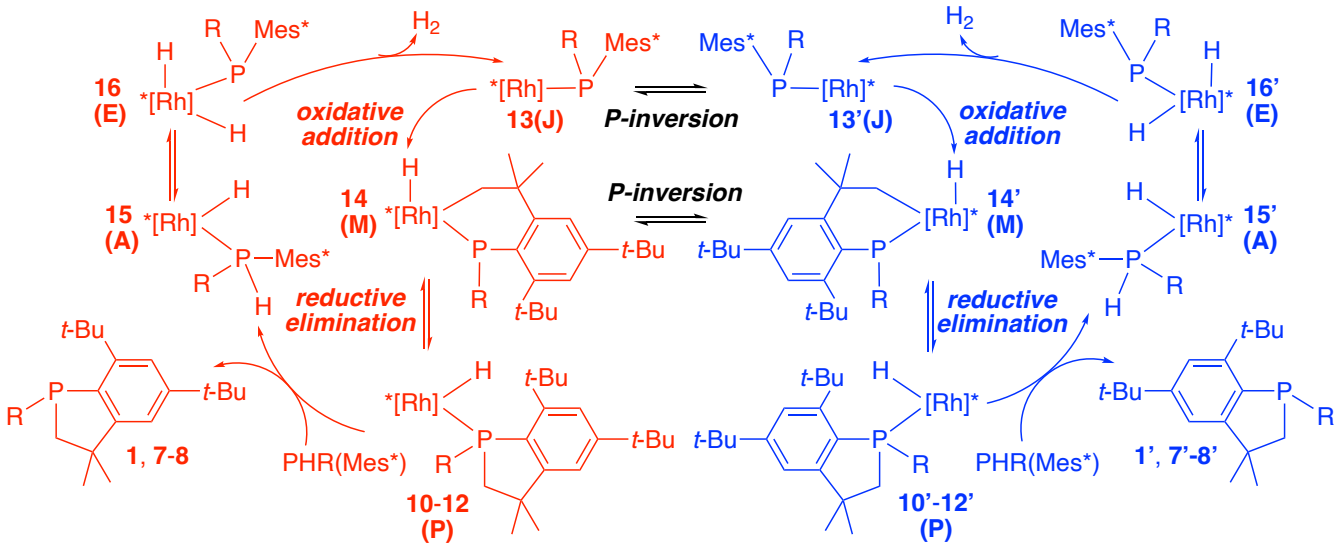

Enantioselectivity in catalysis might occur in the C-H activation and/or P-C reductive elimination steps where the diastereomeric intermediates **13**-**13'** and **14**-**14'** are expected to interconvert rapidly by the pyramidal inversion at P which is typical of metal-phosphido complexes.[25] Thus, the speciation of **13**-**13'** and their relative rates of C-H activation might result in diastereoselective formation of **14**-**14'**. If these intermediates underwent P-C reductive elimination faster than they interconverted, then their diastereomer ratio would be retained in resting states **10**-**12** and **10'**-**12'**, and in the enantiomeric ratio of the products. Alternatively, if Rh(III) hydrides **14**-**14'** interconvert more rapidly than their reductive elimination, then the selectivity of C-H activation is irrelevant, and instead enantioselectivity is determined by the relative amounts of **14**-**14'** and their reductive elimination rates. Thus, the relative rates of the two P-inversion processes, C-H oxidative addition, and P-C reductive elimination are crucial in controlling catalytic enantioselectivity.

DFT Studies of Catalysis Provided More Information on the Mechanisms of Oxidative Addition and Reductive Elimination and Their Stereochemistry (Inversion at P in P-H Oxidative Addition and P-C Reductive Elimination) To address these questions, gas-phase DFT calculations were performed at the B3LYP-D3/LACV3P**+ level using the chiral (*R,R*)-Me-DuPhos ligand. The remote *p*-*t*-Bu group on Mes* was omitted to save some computational time. While there are no crystallographically characterized species available in this system, this level of theory has been successfully benchmarked for similar Rh-P complexes in terms of relative ground state structures, energetics, and kinetic reaction barriers.[16a, 26] Since the reactions do not involve charged species and proceed in relatively non-polar solvents no solvent correction was applied. Full details are provided in the SI.

While the principal objective was to elucidate the observed enantioselectivity, the computed stereochemical features of some steps afforded unusual results.

All structures calculated computationally are labelled using letter designations and are shown with accompanying ChemDraw depictions in Figure 1. The free energy landscape is illustrated in Figure 2. The overall reaction incorporates two fundamental reaction sequences. The first (**A** → **J**), involves phosphine coordination, P-H bond activation, and formation of Rh(I)-phosphido intermediates **J** (**13**-**13'** in Scheme 5) by H_2 elimination. The second entails C-H bond activation from **J**, followed by P-C reductive elimination to generate the final cyclophosphinated product **P** (**10**-**12** in Scheme 5), shown experimentally to be the resting state of the cycle. Figure 2 illustrates that the overall conversion of **A** to **P** (+ H_2) is thermodynamically downhill.

Coordination of the two enantiomers of the starting phosphine PHPh(Mes*) to the chiral [Rh((*R,R*)-Me-DuPhos)H] fragment affords two diastereomeric κ-P complexes **A**. The more stable diastereomer is derived from the (*R*)-enantiomer of the original phosphine. Subsequent intermediates (**C**, **E**, **G**, **I**-**J**, **M**, and **P**) and transition structures **B**‡, **D**‡, **F**‡, **H**‡, **K**‡-**L**‡, and **N**‡-**O**‡ derived from this diastereomer are shown in the right-hand column of Figure 1 and in the red pathway of Figure 2. Structures derived from the other κ-P diastereomer are shown in the left-hand column of Figure 1 and in the blue pathway of Figure 2. Transition structures involving inversion at P must result in crossover between the two diastereomeric pathways, a crucial step in determining overall enantioselectivity, and are shown spanning both columns in Figure 1 and in black in Figure 2. While all minima and transition structures along the red pathway were located computationally, some structures in the early stages of the corresponding blue

pathway did not converge satisfactorily and are labelled as “not located”. However, all structures in the latter, rate limiting (for formation of the resting state), parts of both reaction pathways were located.

P-H activation and H_2 elimination		
	Structures derived from (*S*)-PHPh(Mes*) *(blue in Figure 2)*	Structures derived from (*R*)-PHPh(Mes*) *(red in Figure 2)*
A	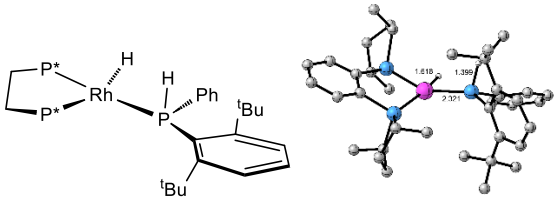	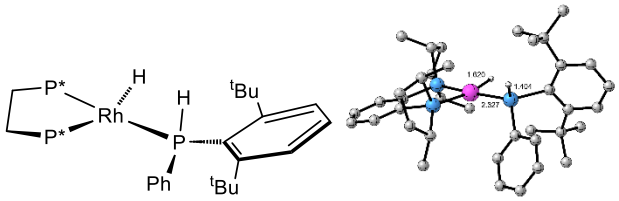
B‡	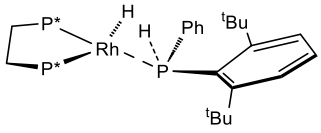 **Not located**	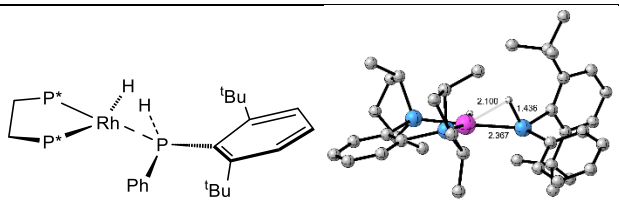
C	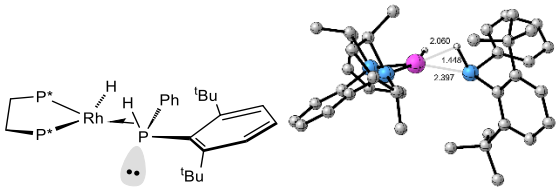	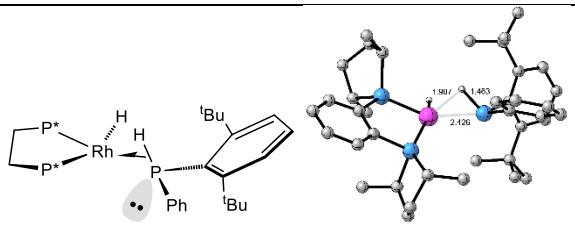
D‡	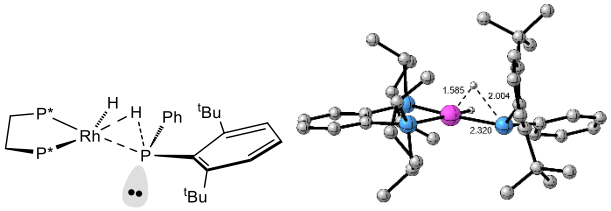	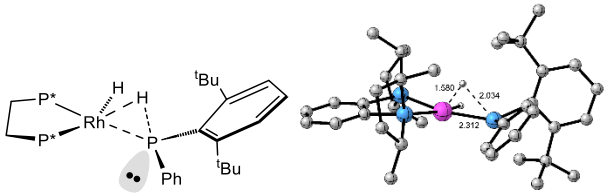
E	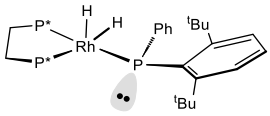 **Not located**	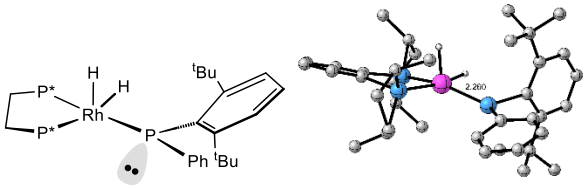
F‡	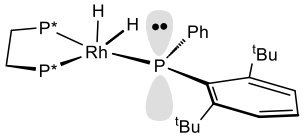 **Not located**	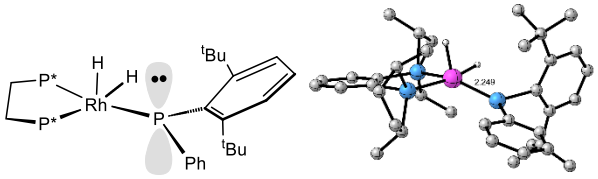
G	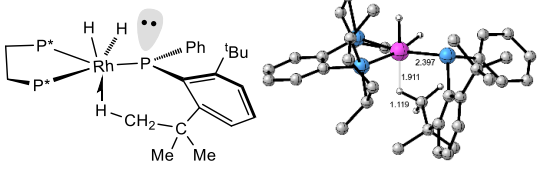	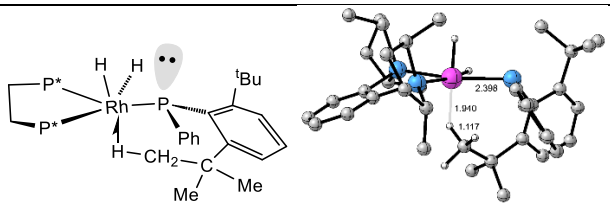
H‡	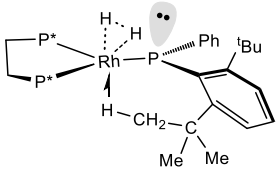 **Not located**	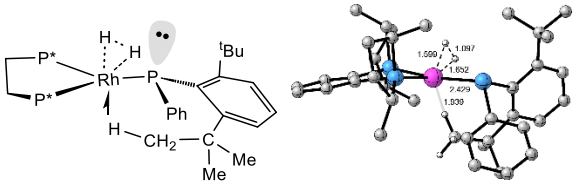

I	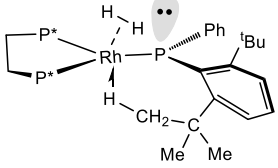	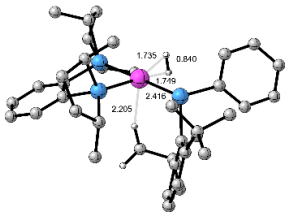	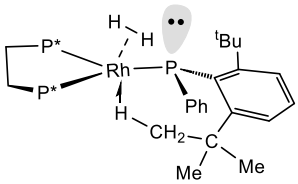	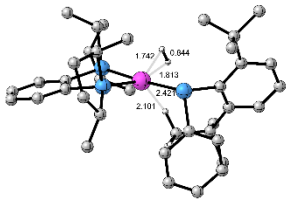
J	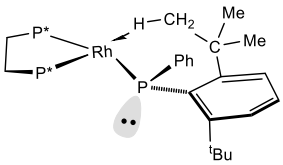	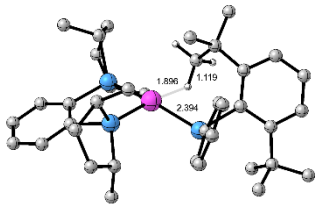	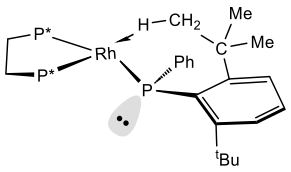	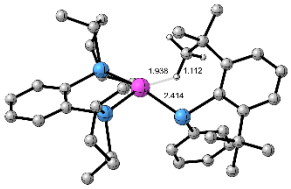
K‡	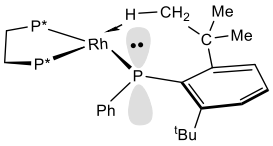	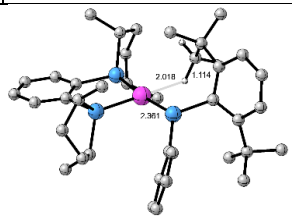		
	C-H activation and P-C elimination			
L‡	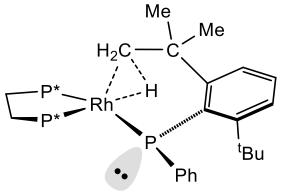	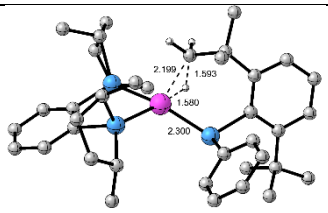	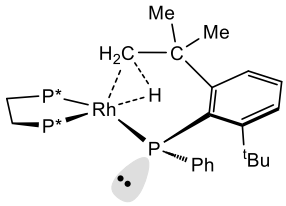	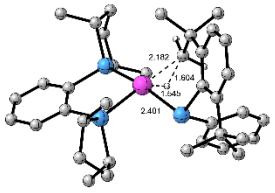
M	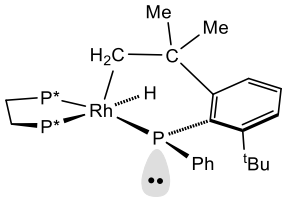	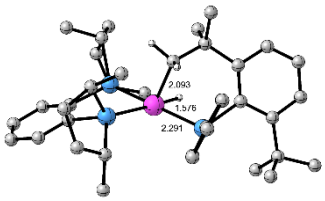	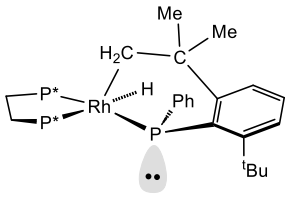	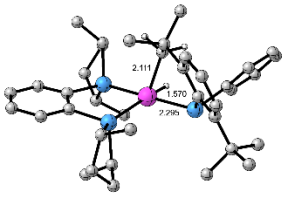
N‡	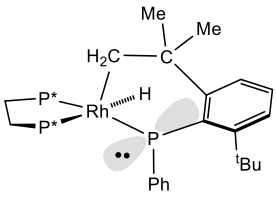	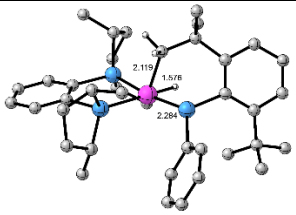		
O‡	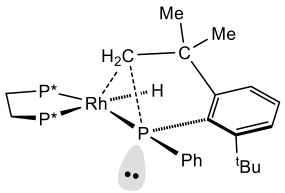	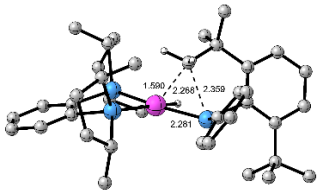	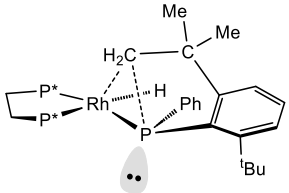	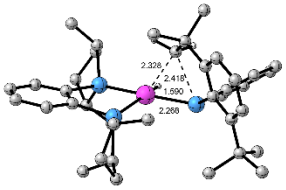
P	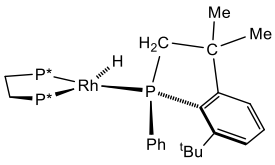	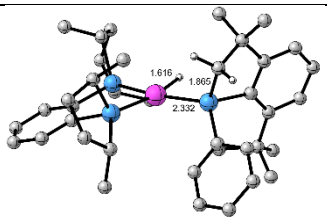	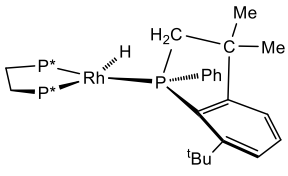	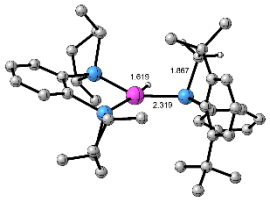

Figure 1. DFT calculated and ChemDraw structures of species **A-P**. Distances are in Å. Transition structures are labelled with a ‡. Most CH-atoms are omitted for clarity, and the *p*-*t*-Bu group of Mes* was omitted in the calculations.

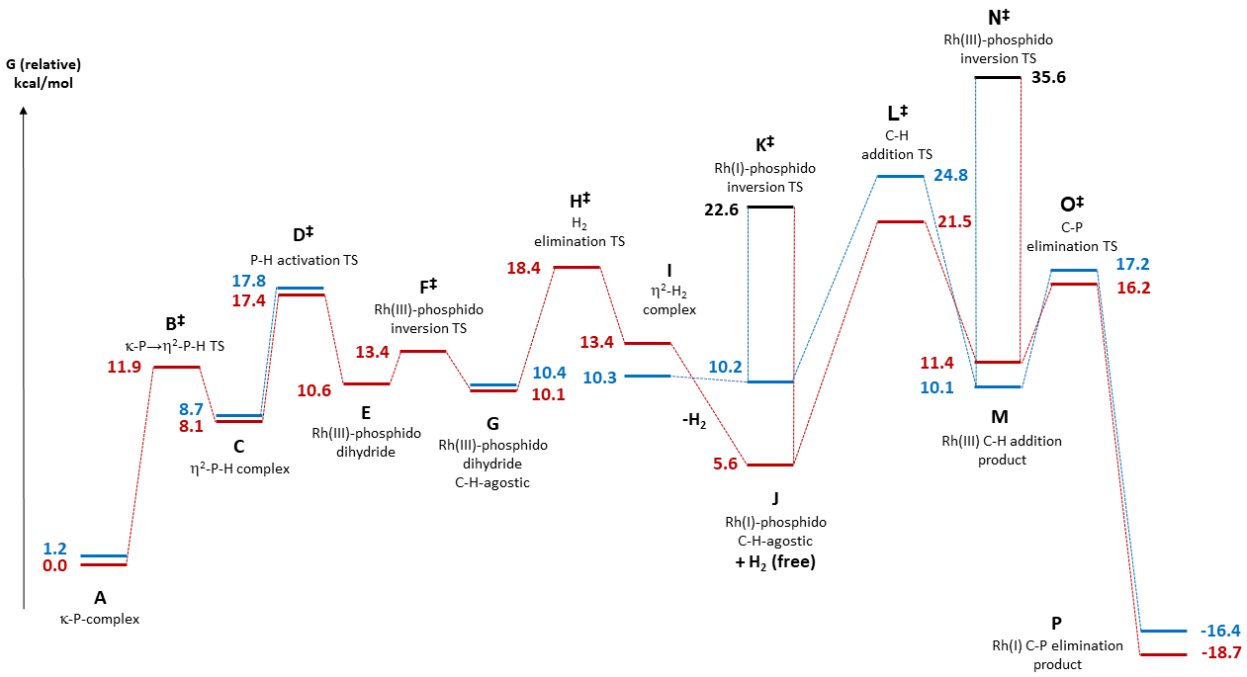

Figure 2. Relative free energy landscape (not to scale) for conversion of diastereomeric κ-P complexes **A** to cyclophosphinated products **P**, with elimination of H_2. All free energies are relative to the more stable diastereomer of **A** as 0.0. To maintain this common zero, relative G-values of **J-P** include a molecule of free H_2.

P-H Activation and H_2 Elimination Proceeded via η^2-PH and η^2-H_2 Complexes Formal oxidative addition of the P-H bond to Rh in **A** is a process which is essential in many previous examples of hydrophosphination and related reactions.[27] This reaction has been examined previously using DFT for P-H addition to Rh(I),[28] Ir(I),[29] and Ru(II)[30] complexes. In each computational study, single transition structures for an apparent one-step migration of H from P to the metal center were located. For example, for systems most closely related to ours, the barrier for oxidative addition of $PHPh_2$ to a Rh(I) precursor has been calculated to be 28.7 kcal/mol,[28] and that for an intramolecular P-H addition in an Ir(I) pincer complex was found to be 24.3 kcal/mol.[29] Here we find computationally that migration of H from P to Rh proceeds in *two steps* from **A** (Figure 2; red pathway) via initial transition structure **B‡** to give an *intermediate η²-PH complex* **C**. This "forward roll" motion of the phosphine corresponds to an intramolecular substitution at Rh of the P lone pair by the P-H σ-bond. This η^2-PH intermediate undergoes a formal oxidative addition of the P-H bond to Rh via transition structure **D‡** to afford phosphido dihydride intermediate **E**. An analogous pathway emanates from the other diastereomer of **A**, but we were unable to locate the corresponding transition structure **B‡**. The barrier for the P-H activation step via transition structures **D‡** is almost identical for both diastereomers. The overall barriers for conversion of the phosphine complex **A** to phosphido dihydride **E** of ca. 18 kcal/mol (which assumes that the non-located energy of the blue **B‡** is similar to that of the red **B‡** and less than that of **D‡**) are somewhat lower than previously calculated for $PHPh_2$ (*vide supra*). Correlation of the structures of **C** and **D‡** (Figure 1) indicates that the overall P-H activation proceeds with *net inversion at P*. An Intrinsic Bond Orbital (IBO) study of this reaction step is presented later.

Intermediate **E**, formed by P-H migration to Rh with inversion at P, could only be located computationally on the red pathway; its low energy P-inversion via transition structure **F‡** allows rapid conversion to **G**, containing a weak agostic interaction with a C-H bond of an *o*-*t*-Bu group. The low energy P-inversion of **E** conceals the fact that **E** is itself formed by inversion at phosphorus. This apparent overall retention at phosphorus has been noted for P-H activation in an Ir(I) pincer complex.[29] The energies of the two diastereomers of **G** are almost identical. Their possible interconversion by P-inversion and Rh-P bond rotation would require sacrificing this agostic interaction; see below for studies on such processes in later intermediates.

Elimination of H_2 from diastereomers **G** occurs via transition structure **H‡** (located on the red pathway) to give dihydrogen complexes **I**. Dissociative loss of H_2 accompanies rotation about the Rh-P bond to afford the Rh(I) intermediates **J** in which the C-H agostic interaction is maintained. Both intermediates **J** are uphill from starting materials (**A**) and the reaction is presumably driven by irreversible loss of gaseous H_2. Unlike preceding intermediates, diastereomers **J** are significantly different in energy, providing a means of enantioselectivity. As found for other phosphido ligands in square planar metal complexes,[25] phosphorus inversion via **K‡** is facile, with barriers of 12.4 and 17.0

kcal/mol for the blue and red pathways. Significantly, P-inversion in **J** affords a direct single-step crossover pathway, without requiring subsequent Rh-P bond rotation. While we cannot discount that phosphido inversion occurs in preceding higher coordination number intermediates **E** or **G**, diastereomer interconversion in these structures requires additional rotation about the Rh-P bond, and that for **G** requires disrupting the agostic CH interaction. These alternative pathways have not been studied computationally.

The significant difference in the energies of diastereomers **J** is likely due to steric interactions between the Ph group of the phosphido ligand and the *cis*-proximal CH_3 group of the chelating Me-DuPhos in each diastereomer, as shown in Figure 3. On the blue pathway, the energy of **J** is raised because Ph occupies the same quadrant of space as the *cis*-proximal CH_3 group; on the red pathway, the Ph group in **J** sits in the vacant quadrant relative to this *cis*-proximal CH_3 group, with the corresponding *trans*-proximal CH_3 further away.

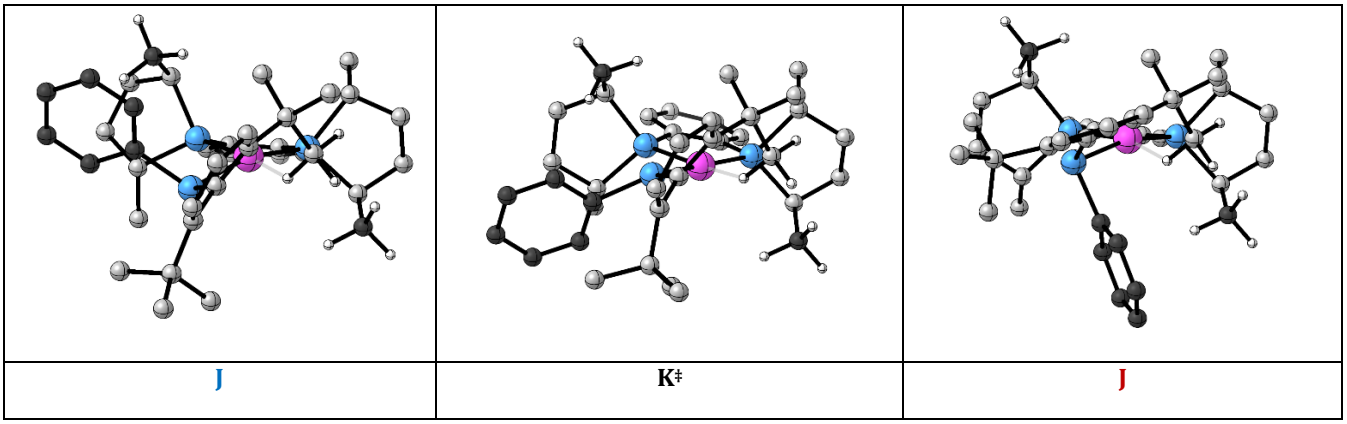

Figure 3. Alternate view of intermediates **J** on the red and blue pathways of Figure 2 and the P-inversion transition structure **K‡** connecting them. The carbons of the phosphido Ph group and the proximal CH_3 groups of the Me-DuPhos chelate are darkened for emphasis.

C-H Bond Activation Occurred via Agostic Intermediates and P-C Reductive Elimination Proceeded with Inversion at P C-H bond activation from agostic intermediates **J**, via transition structures **L‡**, affords intermediates **M**. This step is rate-limiting for the product formation in Figure 2, but slower than catalytic turnover, which is controlled by later ligand substitution. A single step crossover of diastereomers **M** by P-inversion could occur at this stage, but the transition structure **N‡** lies too high in energy, with barriers of 24.2 (red) and 25.5 (blue) kcal/mol, perhaps because the phosphorus is incorporated into a ring. Instead, subsequent C-P reductive elimination occurs via a lower energy transition structure **O‡** to give the final products **P**. Two points are noteworthy: reductive elimination of the P-C bond must occur between apical and basal sites in 5-coordinate **M** to afford a square planar product **P**; and stereochemical correlation of the cyclic structures of **M** and **P** illustrates that, as with P-H oxidative addition, reductive elimination to form the C-P bond must occur with *inversion of configuration at phosphorus*.

Enantioselectivity via C-H Activation Given the relative energetics of this latter sequence, a specific cause of enantioselectivity is difficult to assign. However, it clearly arises in the C-H bond activation sequence, as shown in Scheme 6, which includes a portion of Scheme 5 with a focus on the key steps and their computed barriers from Figure 2. These computational results answer the relative rates question posed in discussion of Scheme 5: P-C reductive elimination in Rh(III) phosphido complexes **14**-**14'** (**M**) via transition structure **O‡** is much faster than P-inversion via **N‡**. Therefore, the relative rates of P-inversion (via **K‡**) and C-H activation (via **L‡**) in Rh(I) phosphido intermediates **J** (**13**-**13'**) control enantioselectivity. Because P-inversion is not much faster than C-H activation in both pathways, the Curtin-Hammett condition does not apply.[31] Instead, blue intermediate **13'** undergoes P-inversion more rapidly than oxidative addition, with barriers of 12.4 and 14.6 kcal/mol, respectively. These relative rates are reversed for red **13**, whose C-H activation barrier of 15.9 kcal/mol is less than that for P-inversion (17.0 kcal/mol), so formation of red Rh-hydride **M** is kinetically favored, leading selectively to the red product **P** after fast reductive elimination.

Scheme 6. A Portion of Scheme 5 Highlighting the Relative Rates of P-Inversion, Oxidative Addition, and P-C Reductive Elimination Steps, with Computed Barriers (kcal/mol) Involving Transition Structures **K**‡, **L**‡, **N**‡, and **O**‡ from Figure 2

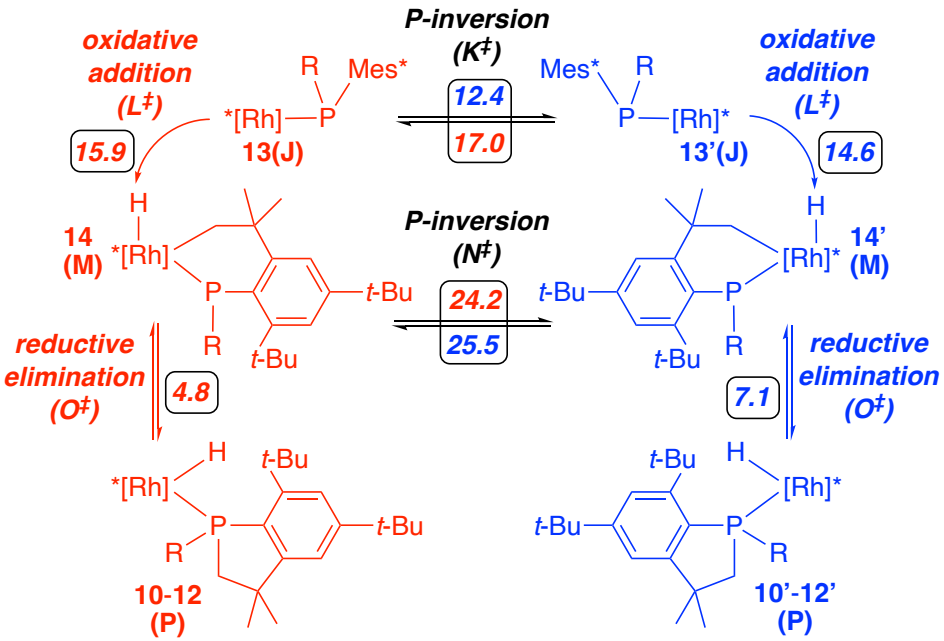

Intrinsic Bond Orbital (IBO) Studies of Bond Cleavage and Formation Steps Showed That Both P-H and C-H Oxidative Addition Involved Element-to-Rh Proton Transfer, Not Hydride Migration Components of this overall reaction sequence allowed further study of three distinct bond cleavage (P-H, C-H) and formation (P-C) reactions using the Intrinsic Bond Orbital (IBO) methodology,[32] which identifies and correlates those orbitals undergoing the largest electron density changes along the reaction coordinate. As a result, electron redistribution along the reaction coordinate can be defined, and used as a basis for an arrow-pushing depiction for each reaction.[33] Only structures on the red pathway were subjected to this methodology.

Figure 4 illustrates the IBOs for the P-H bond activation step **A** → **C** → **E**. Three IBOs dominate the electron flow from **A**; the initial P-H σ-bond, Rh 4d-orbital (a lone-pair on Rh) and Rh-P σ-bond. As shown, the P-H bond electrons evolve into the new Rh-P σ-bond, the Rh d-electrons become the Rh-H σ-bond, and the Rh-P σ-bonding electrons transform into the new P-lone pair of the phosphido ligand. In intermediate **C** the components of the Rh-P-H bonding are consistent with the familiar σ-donation from P-H to Rh and backbonding from Rh to P-H σ* which results in activation of the P-H bond. The "forward roll" of the phosphine ligand from **A** → **C** interchanges the roles of the P lone pair and the P-H σ-bond and brings the P-H bond into closer proximity to the metal, facilitating P-H bond activation. Translation into an arrow pushing picture is shown at the bottom of the Figure. This is clearly not a hydride migration reaction, but a proton transfer from phosphorus to Rh. As suggested by a reviewer, this mechanism is consistent with the more common observation of P-H activation with more acidic arylphosphines than the less acidic alkylphosphines.[27]

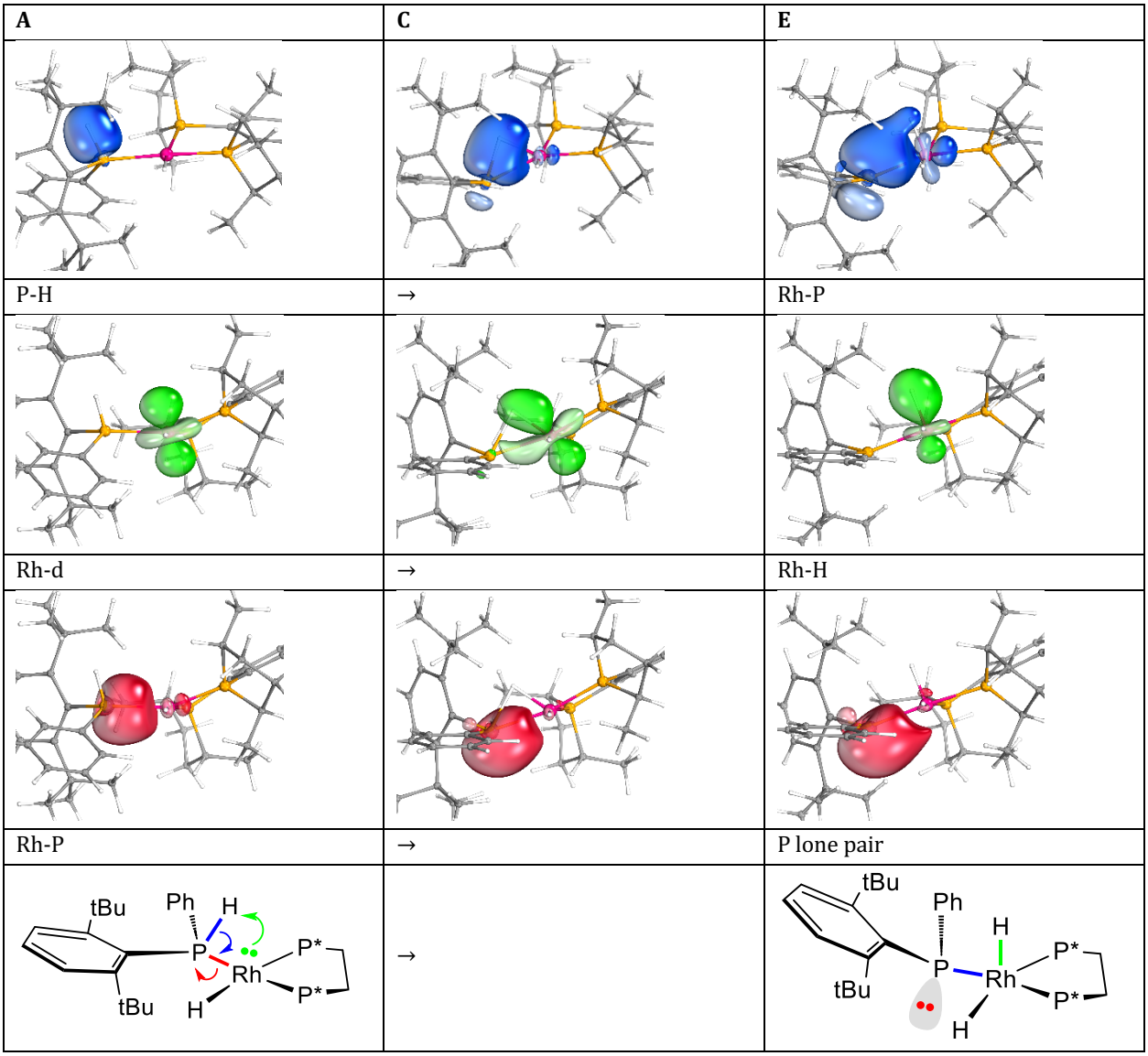

Figure 4. Evolution of IBOs for the P-H bond activation **A** → **C** → **E**, and the corresponding arrow-pushing mechanism. Some peripheral atoms are truncated.

Similarly, electron redistribution in the C-H activation process **J** → **L**‡ → **M** can be tracked as shown in Figure 5. Here the initial C-H bond electrons in the agostic starting material evolve into the new Rh-C σ-bond, while the Rh-d orbital becomes the new Rh-H σ-bond. Once again, proton abstraction from carbon is preferred to hydride migration.

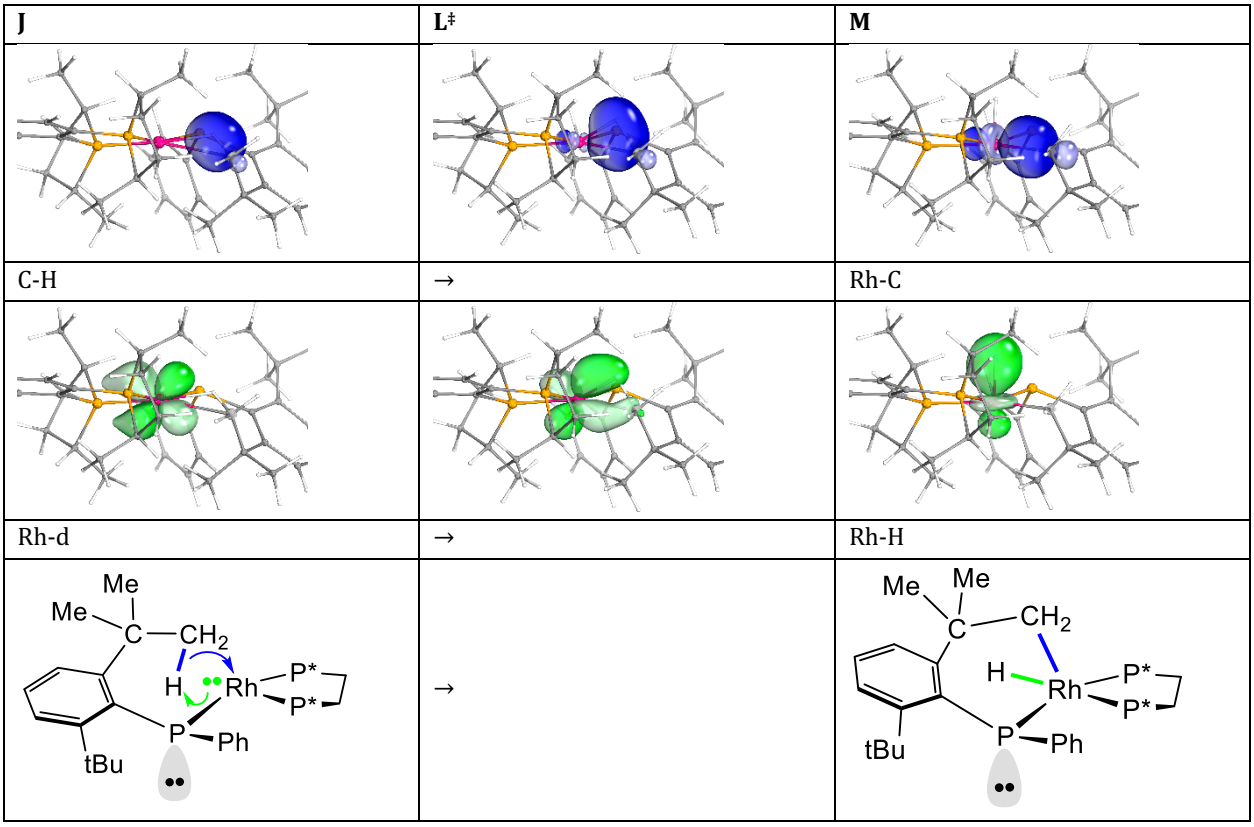

Figure 5. Evolution of IBOs for the P-H bond activation **J** → **L‡** → **M**, and the corresponding arrow-pushing mechanism. Some peripheral atoms are truncated.

Lastly, IBO analysis of the final P-C bond forming step, **M** → **O‡** → **P**, is illustrated in Figure 6. The initial Rh-P σ-bond evolves into the new P-C σ-bond, the Rh-C σ-bond becomes a Rh d-lone pair, and the original P lone pair evolves into the new Rh-P σ-bond. The interchange of the P-C bonding and P-lone pair electron pairs in this reductive elimination results in inversion at P, and is clearly the reverse of that in the P-H bond activation (*vide supra*); i.e., run backwards, P-C bond activation would involve nucleophilic attack by Rh on P.

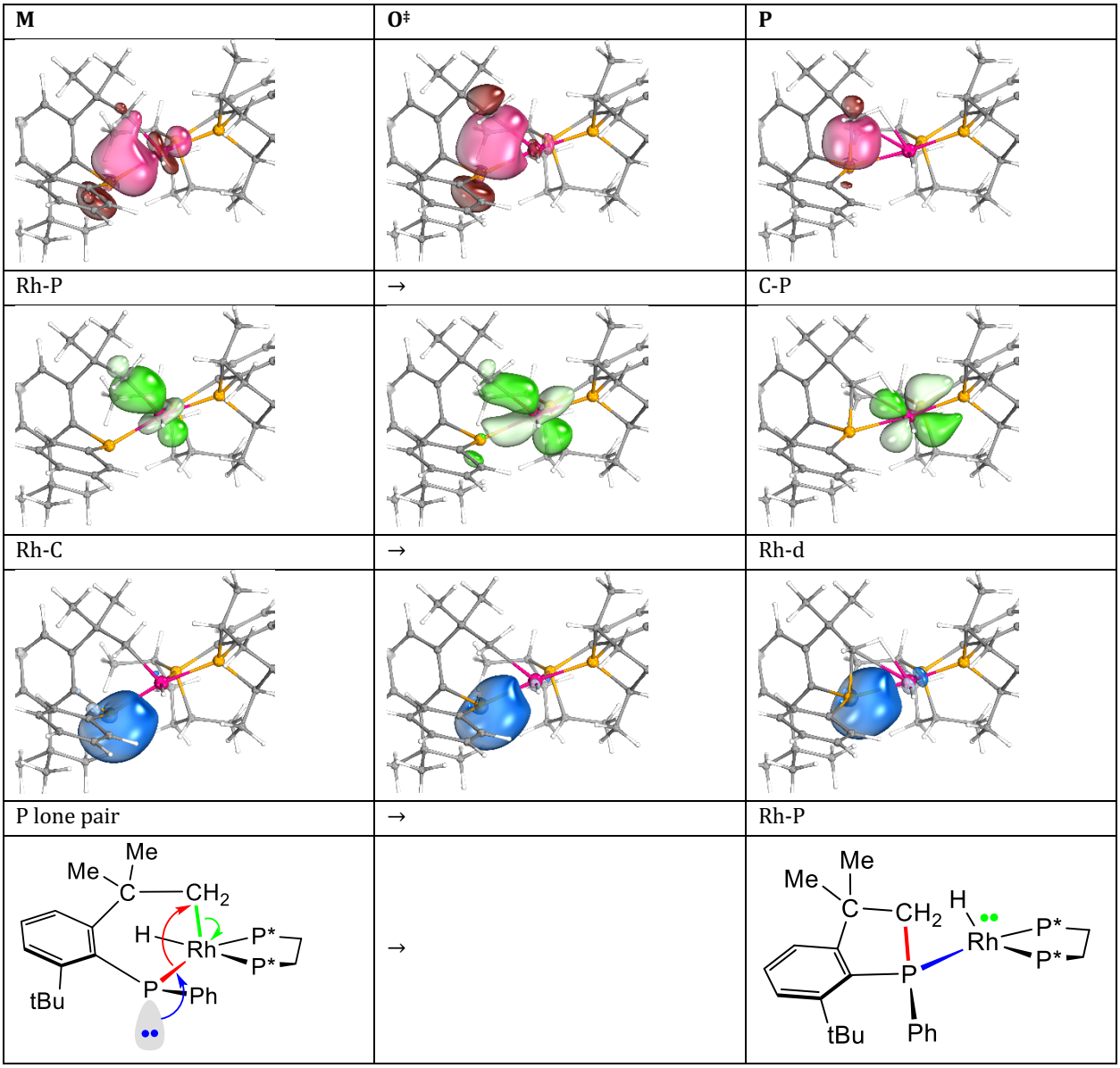

Figure 6. Evolution of IBOs for the P-C bond elimination **M** → **O‡** → **P**, and the corresponding arrow-pushing mechanism. Some peripheral atoms are truncated.

Comparison to Experimental Stereochemistry of Oxidative Addition and Reductive Elimination Involving P-H and P-C Bonds, With Retention of P-Configuration at Four-Coordinate Phosphorus In the very limited experimental studies of these processes (Scheme 7), both P-H oxidative addition of a secondary phosphine oxide to Pt(0)[34] and P-C reductive elimination of a palladium complex with aryl and phosphido-borane ligands occurred with *retention* of configuration at four-coordinate P,[35] consistent with concerted processes. The presence of a P lone pair in formation of **G** and **O**, according to our computational results, leads instead to *inversion* at P in oxidative addition or reductive elimination of a three-coordinate phosphine. The IBO analysis offers a rationalization of this behavior for P-C reductive elimination, which proceeds by nucleophilic attack of the Rh-phosphido bonding electrons at C, assisted by conversion of the P lone pair into a Rh-P bond. Similarly, we computationally observed nucleophilic reactivity in the copper-phosphido complex Cu(triphos)(PPh_2) resulting from the Cu-P bond instead of the P lone pair.[36]

Scheme 7. Experimental Observations of Stereochemistry in P-H Oxidative Addition and P-C Reductive Elimination: Retention of Configuration at Four-Coordinate Phosphorus (Men = (–)-Menthyl)

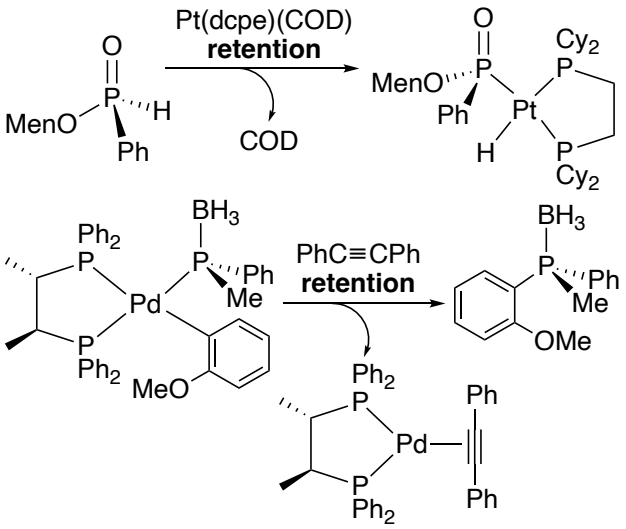

CONCLUSIONS

We have reported a new catalytic asymmetric process for synthesis of P-stereogenic benzophospholanes, along with identification of the resting states and ligand effects on rate and selectivity. Despite the promising enantioselectivity, the slow rate at room temperature, high catalyst loading, and limited scope means that the process is not yet synthetically useful. Catalysis was fastest with the least sterically demanding ligand and the smallest bite angle, consistent with the observation of Rh-hydride resting states **10**-**12** and rate-determining substitution of the product tertiary phosphine by the substrate secondary phosphine at the metal. To promote the presumed associative mechanism for this step, which is common for square planar complexes, further development will focus on smaller chiral ligands with reduced bite angles, or monodentate chiral ligands.

DFT studies suggested that the enantioselective step was C-H activation in the phosphido intermediates Rh(diphos*)(PR(Mes*)) and that both P-H activation and P-C reductive elimination at three-coordinate phosphorus proceeded with inversion at P, in contrast to experimental observations of retention at P in these reactions at four-coordinate phosphorus. IBO studies are consistent with a proton (rather than hydride) transfer to the metal in the P-H and C-H activation steps, which may be more widely relevant in such processes.

EXPERIMENTAL SECTION

General Experimental Details Unless otherwise noted, all reactions and manipulations were performed in dry glassware under a nitrogen atmosphere at ambient temperature in a glove box or using standard Schlenk techniques. Pentane, CH_2Cl_2, and THF were dried over alumina columns similar to those described by Grubbs.[37] NMR spectra were recorded with 500 or 600 MHz spectrometers. ^1H or ^{13}C NMR chemical shifts are reported vs Me_4Si and were determined by reference to the residual ^1H or ^{13}C solvent peaks. ^{31}P NMR chemical shifts are reported vs H_3PO_4 (85%) used as an external reference. Coupling constants are reported in Hz, as absolute values. Unless indicated, peaks in NMR spectra are singlets. Atlantic Microlab provided elemental analyses. Mass spectrometry was performed at the University of Illinois. These reagents were prepared by the literature methods: [Rh((*R,R*)-Me-DuPhos)(Cl)]$_2$,[38] [Rh((*R,R*)-*i*-Pr-DuPhos)(Cl)]$_2$ and other [Rh(diphos*)(Cl)]$_2$ precursors, Rh(COD)(CH_2Ph), and Rh(diphos*)(CH_2Ph),[16a] Co((*R,R*)-*i*-Pr-DuPhos)Cl_2,[39] the Pd-chiral amine complex (*S*)-[Pd($NMe_2CH(Me)C_6H_4$)(Cl)]$_2$,[20a] Mes*Br and PH_2Mes*,[40] PHMe(Mes*) and PHPh(Mes*),[41] and PCl(2,4-(*t*-Bu)$_2C_6H_2$-6-CMe_2CH_2).[8]

General procedure for catalytic dehydrocoupling-cyclophosphination A mixture of the catalyst precursor and the substrate in THF was monitored at room temperature by $^{31}P\{^1H\}$ NMR spectroscopy. Catalyst loading ranged from 9 to 27 mol %, and the amount of substrate from 0.1 to 0.3 mmol; see the SI for details of the individual experiments in Table 1.

Synthesis of the benzophospholane PPh(2,4-(*t*-Bu)$_2C_6H_2$-6-CMe_2CH_2) (8) A solution of PhMgBr (1 M in THF, 3.4 mL, 3.4 mmol, 1.2 equiv) was added to a solution of the chlorophosphine P(2,4-(*t*-Bu)$_2C_6H_2$-6-CMe_2CH_2)(Cl) (1 g, 3.2 mmol, 1 equiv) in 50 mL of THF at -78 °C. The mixture was slowly warmed to room temperature and stirred for 1 h. The solvent was removed under vacuum. The product was extracted with pentane and the resulting solution was filtered over Celite to remove Mg salts. The solvent was removed under vacuum to give 850 mg (75% yield) of a colorless oil which $^{31}P\{^1H\}$ NMR spectroscopy showed contained two minor impurities (about 5% each): the phosphine oxide (see below, 48 ppm), and the secondary phosphine **1** (–79 ppm).[18] According to NMR spectroscopy, this material also contained the arene Mes*H, which was presumably derived from the Mes*Br starting material. ^1H NMR (C_6D_6): δ 7.42 (3H), 1.34 (27H); $^{13}C\{^1H\}$ NMR (C_6D_6): δ 150.4 (quat Ar), 119.7 (Ar CH), 35.1 (quat *C*Me_3), 31.4 (C*Me*$_3$). In a similar smaller-scale procedure, the product was further purified by chromatography on silica with pentane.

HRMS m/z calcd for $C_{24}H_{34}P$: 353.2398. Found: m/z 353.2411. $^{31}P\{^1H\}$ NMR (242.9 MHz, C_6D_6): δ -11.9. ^1H NMR (600 MHz, C_6D_6): δ 7.65 (d, J = 4, 1H, Ar), 7.27 (1H, Ar), 7.22-7.18 (m, 2H, Ar), 6.93-6.92 (m, 3H, Ar), 2.24 (dd, J_{P-H} = 20, J = 14, 1H, CH_2), 1.96 (d, J = 14, 1H, CH_2), 1.57 (9H, CH_3), 1.35 (9H, CH_3), 1.21 (3H, CH_3), 0.97 (3H, CH_3). $^{13}C\{^1H\}$ NMR (150.9 MHz, C_6D_6): δ 159.8 (quat Ar), 153.6 (d, J = 14, quat Ar), 153.2 (quat Ar), 144.6 (d, J = 26, quat Ar), 132.7 (d, J = 16, quat Ar), 132.1 (d, J = 18, Ar CH), 128.1 (d, J = 5, Ar CH, obscured by C_6D_6 signals), 127.7 (Ar CH), 122.2 (d, J = 5, Mes* CH), 119.3 (Mes* CH), 47.2 (d, J = 6, quat CMe_2), 43.3 (d, J = 9, CH_2), 37.6 (quat CMe_3), 35.2 (quat CMe_3), 33.3 (d, J = 4, CH_3), 32.4 (d, J = 9, CH_3), 31.8 (CH_3), 31.7 (CH_3).

Synthesis of PPh(O)(2,4-(*t*-Bu)$_2C_6H_2$-6-CMe_2CH_2) (9) A solution of aqueous H_2O_2 (100 μL, 30% v/v, 1.3 equiv) was added to a stirring solution of the phosphine PPh(2,4-(*t*-Bu)$_2C_6H_2$-6-CMe_2CH_2) (150 mg, 0.42 mmol, 1 equiv) in 2

mL of THF at room temperature. After 30 min, $^{31}P\{^{1}H\}$ NMR spectroscopy showed that most of the phosphine was oxidized; full conversion was seen after 3 d. The solvent was removed under vacuum to give a colorless oil (140 mg). This material contained Mes*H, as in the phosphine precursor. When the oil was triturated and left overnight in pentane at room temperature, a white solid precipitated (72 mg, 46% yield).

HRMS m/z calcd for $C_{24}H_{34}OP$: 369.2347. Found: m/z 369.2352. $^{31}P\{^{1}H\}$ NMR (242.9 MHz, C_6D_6): δ 51.9. ^{1}H NMR (600 MHz, C_6D_6): δ 7.66-7.60 (d, J = 4, 1H, Ar), 7.60-7.53 (m, 2H, Ar), 7.29 (d, J = 13, 1H, Ar), 7.00-6.90 (m, 3H, Ar), 2.36 (d, J = 18, 1H, CH_2), 1.98 (dd, J = 7, 14, 1H, CH_2), 1.51 (9H, CH_3), 1.35 (3H, CH_3, Mes*H), 1.27 (9H, CH_3), 1.18 (3H, CH_3), 1.05 (3H, CH_3). $^{13}C\{^{1}H\}$ NMR (150.9 MHz, C_6D_6): δ 159.8 (d, J = 29, quat Ar), 156.6 (quat Ar), 155.5 (d, J = 6, quat Ar), 139.5 (quat Ar), 138.6 (d, J = 3, quat Ar), 131.2 (d, J = 10, Ar CH), 128.6 (d, J = 3, Ar CH), 128.5 (d, J = 3, Ar CH), 123.8 (d, J = 9, Mes* CH), 118.9 (d, J = 14, Mes* CH), 43.9 (d, J = 73, CH_2), 33.8 (d, J = 9, CH_3), 32.6 (d, J = 2, CH_3), 31.8 (Mes*H), 31.4-31.3 (d, J = 4, CH_3), 31.3 (CH_3).

[Rh((*R,R*)-Me-DuPhos)(Cl)]$_2$ catalyzed dehydrocoupling-cyclophosphination of PHPh(Mes*) (Table 1, entry 7). An orange solution of [Rh((*R,R*)-Me-DuPhos)(Cl)]$_2$ (20 mg, 0.023 mmol, 1 equiv), PHPh(Mes*) (80 mg, 0.23 mmol, 5 equiv per Rh), and $NaOSiMe_3$ (5 mg, 0.045 mmol, 2 equiv) in 2 mL of THF was monitored via $^{31}P\{^{1}H\}$ NMR spectroscopy. Full conversion was observed after 3 d at room temperature and 30% aqueous H_2O_2 was added (33 μL, 0.34 mmol, 1.3 equiv). The dark red sample immediately lightened to a yellow green. The solvent was then removed under vacuum and the residue was dissolved in 2 mL of ethyl acetate. The rhodium was removed via chromatography on a pipette column of silica (0.5 cm x 5 cm). The eluant was concentrated under vacuum to give a clear oil. NMR spectroscopy in C_6D_6 showed a mixture of phosphine **8** and phosphine oxide **9**. The solution was left in air overnight and showed full conversion to the tertiary phosphine oxide, according to $^{31}P\{^{1}H\}$ NMR spectroscopy. Removing the solvent under vacuum and triturating with pentane gave a white solid after drying (53 mg, 63% yield). A solution of *S*-Fmoc-Trp(Boc)-OH (153 mg, 0.29 mmol, 2 equiv) in 1 mL of C_6D_6 was added. The er (85:15) was measured by comparing the ratio of signals centered at 55 ppm in the $^{31}P\{^{1}H\}$ NMR spectrum (see the SI).

Generation of the resting state Rh((*R,R*)-*i*-Pr-DuPhos)(PH(2,4-(*t*-Bu)$_2$C$_6$H$_2$-6-CMe$_2$CH$_2$)(H) (10a) from PH$_2$Mes* with the precursor Rh((*R,R*)-*i*-Pr-DuPhos)(CH$_2$Ph) Crude Rh((*R,R*)-*i*-Pr-DuPhos)(CH_2Ph) (25.7 mg, 0.035 mmol, 1 equiv, containing COD) was added to PH_2Mes* (16.5 mg, 0.035 mmol, 1 equiv) in 2 mL of THF resulting in an orange-brown solution. The solvent was removed under vacuum and the resulting orange-brown solid was dissolved in C_6D_6 for characterization. The $^{31}P\{^{1}H\}$ NMR spectrum showed a 2:1 mixture of diastereomers. The ^{1}H NMR spectrum showed two overlapping hydride signals. See Table 2 for selected NMR data and the SI for spectra.

Generation of the resting state Rh((*R,R*)-*i*-Pr-DuPhos)(PPh(2,4-(*t*-Bu)$_2$C$_6$H$_2$-6-CMe$_2$CH$_2$)(H) (12a) from PHPh(Mes*) with the precursor Rh((*R,R*)-*i*-Pr-DuPhos)(CH$_2$Ph) A solution of crude Rh(COD)(CH_2Ph) (44 mg, 0.14 mmol, 1 equiv) in 2 mL of THF was cooled to -78 °C. A solution of (*R,R*)-*i*-Pr-DuPhos (57 mg, 0.14 mmol, 1 equiv) in 4 mL of THF was added via cannula, followed by PHPh(Mes*) (53 mg, 0.14 mmol, 1 equiv). After one week at room temperature, the $^{31}P\{^{1}H\}$ NMR spectrum showed formation of phosphine 8 (–11.8 ppm) and remaining starting material (–65.0 ppm), as well as signals assigned to Rh((*R,R*)-*i*-Pr-DuPhos)(PPh(2,4-(*t*-Bu)$_2$C$_6$H$_2$-6-CMe$_2$CH$_2$))(H) (**12a**) and unidentified impurities (δ 57.8, 41.5). See Table 2 for selected NMR data and the SI for spectra.

Generation of the resting state Rh((*R,R*)-*i*-Pr-DuPhos)(PPh(2,4-(*t*-Bu)$_2$C$_6$H$_2$-6-CMe$_2$CH$_2$)(H) (12a) from PHPh(Mes*) with the precursor [Rh((*R,R*)-*i*-Pr-DuPhos)(Cl)]$_2$ and NaOSiMe$_3$ [Rh((*R,R*)-*i*-Pr-DuPhos)(Cl)]$_2$ (111 mg, 0.10 mmol) was treated with PHPh(Mes*) (75 mg, 0.21 mmol) and $NaOSiMe_3$ (23 mg, 0.20 mmol) in 1 mL of C_6D_6 to give an orange solution containing Rh((*R,R*)-*i*-Pr-DuPhos)(PPh(2,4-(*t*-Bu)$_2$C$_6$H$_2$(6-CMe$_2$CH$_2$))(H) (12a) as the major product as a 7:1 mixture of diastereomers, according to $^{31}P\{^{1}H\}$ NMR integration, plus PPh(2,4-(*t*-Bu)$_2$C$_6$H$_2$(6-CMe$_2$CH$_2$)) (8) and its oxide PPh(O)(2,4-(*t*-Bu)$_2$C$_6$H$_2$(6-CMe$_2$CH$_2$)) (9) as minor components. The Rh complex was characterized in the mixture by multinuclear spectroscopy. See Table 2 for selected NMR data and the SI for spectra.

ASSOCIATED CONTENT

Supporting Information

The Supporting Information is available free of charge on the ACS Publications website.

Additional experimental details, NMR spectra, and computational results (PDF)

Computed structures (xyz)

AUTHOR INFORMATION

Corresponding Authors

* glueck@dartmouth.edu
* russell.p.hughes@dartmouth.edu

The authors declare no competing financial interests.

ACKNOWLEDGMENT

We thank the National Science Foundation (CHE-1954412 and CHE-1562037) for support. This manuscript is dedicated to our colleagues David Lemal and Thomas Spencer on the occasion of their 90th birthdays.

REFERENCES

1. (a) Kadyrov, R.; Monsees, A. Practical routes to chiral phospholanes. In *Phosphorus Ligands in Asymmetric Catalysis*, Börner, A. Ed.; Vol. 3; Wiley-VCH, 2008; pp 1234-1243. (b) Clark, T.; Landis, C. Recent Developments in Chiral Phospholane Chemistry. *Tetrahedron: Asymmetry* **2004**, *15*, 2123-2137. (c) Burk, M. J. Modular Phospholane Ligands in Asymmetric Catalysis. *Acc. Chem. Res.* **2000**, *33*, 363-372. (d) Mei, P.; Ma, Z.; Chen, Y.; Wu, Y.; Hao, W.; Fan, Q.-H.; Zhang, W.-X. Chiral bisphosphine Ph-BPE ligand: a rising star in asymmetric synthesis. *Chem. Soc. Rev.* **2024**, *53*, 6735-6778.

2. (a) Imamoto, T. P-Stereogenic Phosphorus Ligands in Asymmetric Catalysis. *Chem. Rev.* **2024**, *124*, 8657–8739. (b) Tang, W.; Zhang, X. A Chiral 1,2-Bisphospholane Ligand with a Novel Structural Motif: Applications in Highly Enantioselective Rh-Catalyzed Hydrogenations. *Angew. Chem. Int. Ed.* **2002**, *41*, 1612-1614.

3. Liu, D.; Zhang, X. Practical P-Chiral Phosphane Ligand for Rh-Catalyzed Asymmetric Hydrogenation. *Eur. J. Org. Chem.* **2005**, 646-649.

4. Shimizu, H.; Saito, T.; Kumobayashi, H. Synthesis of Novel Chiral Benzophospholanes and Their Application in Asymmetric Hydrogenation. *Adv. Synth. Catal.* **2003**, *345*, 185-189.

5. Xu, G.; Senanayake, C. H.; Tang, W. P-Chiral Phosphorus Ligands Based on a 2,3-Dihydrobenzo[d][1,3]oxaphosphole Motif for Asymmetric Catalysis. *Acc. Chem. Res.* **2019**, *52*, 1101-1112.

6. For examples of P-stereogenic benzophospholanes, see: (a) Imamoto, T.; Yoshizawa, T.; Hirose, K.; Wada, Y.; Masuda, H.; Yamaguchi, K.; Seki, H. Synthesis and Properties of Optically Active Phosphine-Boranes Possessing an L-Menthyloxy Group. *Heteroat. Chem.* **1995**, *6*, 99-104. (b) Brunker, T. J.; Anderson, B. J.; Blank, N. F.; Glueck, D. S.; Rheingold, A. L. Enantioselective Synthesis of P-Stereogenic Benzophospholanes via Palladium-Catalyzed Intramolecular Cyclization. *Org. Lett.* **2007**, *9*, 1109-1112. (c) Anderson, B. J.; Guino-o, M. A.; Glueck, D. S.; Golen, J. A.; DiPasquale, A. G.; Liable-Sands, L. M.; Rheingold, A. L. Platinum-Catalyzed Enantioselective Tandem Alkylation/Arylation of Primary Phosphines. Asymmetric Synthesis of P-Stereogenic 1-Phosphaacenaphthenes. *Org. Lett.* **2008**, *10*, 4425–4428. (d) Wang, G.; Guino-o, M. A.; Glueck, D. S.; Golen, J. A.; Daley, C. J. A.; Rheingold, A. L. Synthesis of a Phosphapyracene via Metal-Mediated Cyclization: Structural and Reactivity Effects of Acenaphthene Precursors. *Dalton Trans.* **2015**, *44*, 9943–9954. (e) Mohar, B.; Čusak, A.; Modec, B.; Stephan, M. P-Stereogenic Phospholanes or Phosphorinanes from o-Biarylylphosphines: Two Bridges Not Too Far. *J. Org. Chem.* **2013**, *78*, 4665-4673. (f) Rast, S.; Mohar, B.; Stephan, M. Efficient Asymmetric Syntheses of 1-Phenyl-phosphindane, Derivatives, and 2- or 3-Oxa Analogues: Mission Accomplished. *Org. Lett.* **2014**, *16*, 2688–2691 (g) Gschwend, B.; Pugin, B.; Bertogg, A.; Pfaltz, A. P-Chiral Ferrocenephospholanes: Synthesis, Reactivity, Metal Complex Chemistry and Application in the Asymmetric Hydrogenation of Olefins. *Chem. Eur. J.* **2009**, *15* 12993-13007. (h) Fernández-Pérez, H.; Vidal-Ferran, A. Stereoselective Catalytic Synthesis of P-Stereogenic Oxides via Hydrogenative Kinetic Resolution. *Org. Lett.* **2019**, *21*, 7019–7023. (i) Carr, D. J.; Kudavalli, J. S.; Dunne, K. S.; Müller-Bunz, H.; Gilheany, D. G. Synthesis of 2,3-Dihydro-1-phenylbenzo[b]phosphole (1-Phenylphosphindane) and Its Use as a Mechanistic Test in the Asymmetric Appel Reaction: Decisive Evidence against Involvement of Pseudorotation in the Stereoselecting Step. *J. Org. Chem.* **2013**, *78*, 10500–10505. (j) Liu, B.; Liu, P.; Wang, X.; Feng, F.; Wang, Z.; Yang, W. Copper-Catalyzed Dynamic Kinetic Resolution of Secondary Phosphine Oxides. *Org. Lett.* **2023**, *25*, 2178-2183. (k) Wang, X.; Liu, B.; Ge, L.; Hou, S.; Liu, M.; Yang, W. Enantioselective Synthesis of Five to Eight-Membered P-Stereogenic Benzo-Fused Heterocycles via Copper-Catalyzed Dynamic Kinetic Resolution. *Adv. Synth. Catal.* **2024**, *366*, 2285-2291.

7. Stradiotto, M.; Fujdala, K. L.; Tilley, T. D. Generation and Reactivity of {(ethane-1,2-diyl)bis[diisopropylphosphine-κP]}-{[2,4,6-tri(*tert*-butyl)phenyl]phosphino-κP}rhodium ([Rh{PH(^{t}Bu$_3$C$_6$H$_2$)}(^{i}Pr$_2$PCH$_2$CH$_2$P^{i}Pr$_2$)]): Catalytic C-P Bond Formation via Intramolecular C-H/P-H Dehydrogenative Cross-coupling. *Helv. Chim. Acta.* **2001**, *84*, 2958-2970.

8. Yoshifuji, M.; Shima, I.; Ando, K.; Inamoto, N. Thermal Reactions of (2,4,6-tri-tert-butylphenyl)phosphonous dichloride and its Derivatives; Formation of 2,3-dihydro-1H-phosphindoles. *Tetrahedron Lett.* **1983**, *24*, 933-936.

9. (a) Yoshifuji, M.; Sato, T.; Inamoto, N. Wavelength- and Temperature-dependent Photolysis of a Diphosphene. Generation of 2,4,6-tri-t-butylphenylphosphinidene and E/Z Isomerization. *Chem. Lett.* **1988**, 1735-1738. (b) Cowley, A. H.; Gabbai, F.; Schluter, R.; Atwood, D. New Approaches to the Generation of Phosphinidenes. *J. Am. Chem. Soc.* **1992**, *114*, 3142-3144. (c) Alexander, J. B.; Glueck, D. S.; Yap, G. P. A.; Rheingold, A. L. Synthesis, Structure, and Reactivity of the First Phosphaazaallene-Metal Complex. *Organometallics* **1995**, *14*, 3603-3606.

10. (a) Lindner, E.; Weiß, G. A. Oxidative Addition einer C–H-Bindung an ein zweifach koordiniertes Phosphenium-Kation. *Chem. Ber.* **1986**, *119*, 3208-3211. (b) Karsch, H. H.; Reisacher, H.-U.; Müller, G. A 2-Phosphonio-Substituted 1-Phospha-1-alkene: Resonance between P^{III} Alkene and P^{V} Ylide. *Angew. Chem. Int. Ed. Engl.* **1986**, *25*, 454-455. (c) Tsang, C.-W.; Rohrick, C. A.; Saini, T. S.; Patrick, B. O.; Gates, D. P. Reactions of Electrophiles with the Phosphaalkene Mes*P=CH_2: Mechanistic Studies of a Catalytic Intramolecular C−H Bond Activation Reaction. *Organometallics* **2002**, *21*, 1008-1010. (d) Tsang, C.-W.; Rohrick, C. A.; Saini, T. S.; Patrick, B. O.; Gates, D. P. Destiny of Transient Phosphenium Ions Generated from the Addition of Electrophiles to Phosphaalkenes: Intramolecular C-H Activation, Donor-Acceptor Formation, and Linear Oligomerization. *Organometallics* **2004**, *23*, 5913-5923. (e) Tipker, R. M.; Muldoon, J. A.; Jo, J.; Connors, C. S.; Varga, B. R.; Hughes, R. P.; Glueck, D. S. Protonation of P-Stereogenic Phosphiranes: Phospholane Formation via Ring Opening and C–H Activation. *ACS Omega* **2023**, *8*, 12565-12572.

11. (a) David, M.-A.; Paisner, S. N.; Glueck, D. S. Rhodium-Mediated Stoichiometric P=C Bond Cleavage and Catalytic Isomerization in Phosphacumulenes. *Organometallics* **1995**, *14*, 17-19. (b) David, M.-A.; Alexander, J. B.; Glueck, D. S.; Yap, G. P. A.; Liable-Sands, L. M.; Rheingold, A. L. Phosphaazaallene Dimerization and Phosphaallene Isomerization: Catalysis by Zerovalent Palladium and Platinum Complexes. *Organometallics* **1997**, *16*, 378-383. (c) Houdard, R.; Mezailles, N.; Le Goff, X.-F.; Le Floch, P. Platinum(0)-Catalyzed Intramolecular Addition of a C-H Bond onto the P-C Bond of a Phosphaalkene. *Organometallics* **2009**, *28*, 5952-5959.

12. Rojo, P.; Riera, A.; Verdaguer, X. Bulky P-stereogenic ligands. A success story in asymmetric catalysis. *Coord. Chem. Rev.* **2023**, *489*, 215192.

13. Han, L.-B.; Tilley, T. D. Selective Homo- and Heterodehydrocouplings of Phosphines Catalyzed by Rhodium Phosphido Complexes. *J. Am. Chem. Soc.* **2006**, *128*, 13698-13699.

14. (a) Bonanno, J. B.; Wolczanski, P. T.; Lobkovsky, E. B. Arsinidene, Phosphinidene and Imide Formation via 1,2-hydrogen elimination from $(silox)_3Ta(H)EHPh$: Structures of $(silox)_3Ta{=}EPh$ (E=N,P, As). *J. Am. Chem. Soc.* **1994**, *116*, 11159-11160. (b) Hulley, E. B.; Bonanno, J. B.; Wolczanski, P. T.; Cundari, T. R.; Lobkovsky, E. B. Pnictogen-Hydride Activation by $(silox)_3Ta$ (silox = $^tBu_3SiO$); Attempts to Circumvent the Constraints of Orbital Symmetry in N_2 Activation. *Inorg. Chem.* **2010**, *49*, 8524–8544. (c) Hickey, A. K.; Munoz, S. B.; Lutz, S. A.; Pink, M.; Chen, C.-H.; Smith, J. M. Arrested α-hydride migration activates a phosphido ligand for C-H insertion. *Chem. Commun.* **2017**, *53*, 412-415. (d) Pagano, J. K.; Ackley, B. J.; Waterman, R. Evidence for Iron-Catalyzed α-Phosphinidene Elimination with Phenylphosphine. *Chem. Eur. J.* **2018**, *24*, 2554-2557.

15. Glueck, D. S. Metal-Catalyzed Asymmetric Synthesis of P-Stereogenic Phosphines. *Synlett* **2007**, 2627-2634.

16. (a) Scheetz, P. M.; Chachula, S. T.; Hughes, R. P.; Glueck, D. S.; Moore, C. E.; Gembicky, M.; Rheingold, A. L. Synthesis, Structure, Dynamics, and Enantioface-Selective η^3-Benzyl Coordination in the Chiral Rhodium Complexes Rh(diphos*)(η^3-CH_2Ph). *Organometallics* **2020**, *39*, 3802–3816. (b) Chachula, S. T.; Scheetz, P. M.; Zureick, A. H.; Hughes, R. P.; Glueck, D. S.; Hernandez, R. E.; Figueroa, J. S.; Rheingold, A. L. Rhodium-Catalyzed Asymmetric Dehydrocoupling: Enantioselective Synthesis of a P-Stereogenic Diphospholane with Mistake-Correcting Diastereoselectivity. *Organometallics* **2023**, *42*, 1448–1453.

17. (a) Kim, Y. B.; Kim, D.; Dighe, S. U.; Chang, S.; Park, J.-W. Cobalt-Hydride-Catalyzed Hydrosilylation of 3-Alkynes Accompanying π-Bond Migration. *ACS Catal.* **2021**, *11*, 1548-1553. (b) Friedfeld, M. R.; Zhong, H.; Ruck, R. T.; Shevlin, M.; Chirik, P. J. Cobalt-catalyzed asymmetric hydrogenation of enamides enabled by single-electron reduction. *Science* **2018**, *360*, 888-893.

18. For the secondary phosphine **1**, see: (a) Cowley, A. H.; Pakulski, M. Sulfur Cleavage of a Phosphorus-Phosphorus Double Bond. *Tetrahedron Lett.* **1984**, *25*, 2125-2126. (b) Yoshifuji, M.; Sato, T.; Inamoto, N. Wavelength- and Temperature-dependent Photolysis of a Diphosphene. Generation of 2,4,6-tri-t-butylphenylphosphinidene and E/Z Isomerization. *Chem. Lett.* **1988**, 1735-1738. (c) For the P-Me tertiary phosphine **7**, see refs 10c-d.

19. (a) Li, Y.; Raushel, F. M. Differentiation of Chiral Phosphorus Enantiomers by ^{31}P and ^1H NMR Spectroscopy Using Amino Acid Derivatives as Chemical Solvating Agents. *Tetrahedron: Asymmetry* **2007**, *18*, 1391-1397. (b) Chapp, T. W.; Glueck, D. S.; Golen, J. A.; Moore, C. E.; Rheingold, A. L. Platinum-Catalyzed Asymmetric Alkylation of Bis(isitylphosphino)ethane: Stereoselectivity Reversal in Successive Formation of Two P-C Bonds. *Organometallics* **2010**, *29*, 378-388. (c) Chapp, T. W.; Schoenfeld, A. J.; Glueck, D. S. Effects of Linker Length on the Rate and Selectivity of Platinum-Catalyzed Asymmetric Alkylation of the Bis(isitylphosphino)alkanes $IsHP(CH_2)_nPHIs$ (Is = 2,4,6-(i-Pr)$_3C_6H_2$, n = 1–5).

Organometallics **2010**, *29*, 2465-2473. (d) Xu, Z.; Cain, M. F.; Rupert, A. V.; Glueck, D. S.; Golen, J. A.; Rheingold, A. L. Selective formation of a C_3-symmetric P-stereogenic tris(phosphine) via platinum-catalyzed asymmetric alkylation of a tris(secondary phosphine). *Tetrahedron: Asymmetry* **2015**, *26*, 1459–1468.

20. (a) Tani, K.; Brown, L. D.; Ahmed, J.; Ibers, J. A.; Nakamura, A.; Otsuka, S.; Yokota, M. Chiral Metal Complexes. 4. Resolution of Racemic Tertiary Phosphines with Chiral Palladium(II) Complexes. The Chemistry of Diastereomeric Phosphine Palladium(II) Species in Solution, and the Absolute Configuration of [(*S*)-Isopropyl-*tert*-butylphenylphosphine]-[(*R*)-N,N-dimethyl-α-(2-naphthyl)-ethylamine-3*C,N*]chloropalladium(II) Determined by X-Ray Diffraction. *J. Am. Chem. Soc.* **1977**, *99*, 7876-7886. (b) Glueck, D. S. Applications of ^{31}P NMR Spectroscopy in Development of M(Duphos)-Catalyzed Asymmetric Synthesis of P-Stereogenic Phosphines (M = Pt or Pd). *Coord. Chem. Rev.* **2008**, *252*, 2171-2179. (c) Wild, S. B. Resolutions of Tertiary Phosphines and Arsines with Orthometallated Palladium(II)-Amine Complexes. *Coord. Chem. Rev.* **1997**, *166*, 291-311.

21. (a) Bader, A.; Nullmeyers, T.; Pabel, M.; Salem, G.; Willis, A. C.; Wild, S. B. Stereochemistry and Stability of Free and Coordinated Secondary Phosphines. Crystal and Molecular Structure of *[PtCl{1,2-C_6H_4(PMePh)$_2$}(PHMePh)]$PF_6 \cdot CH_2Cl_2$. *Inorg. Chem.* **1995**, *34*, 384-389. (b) Bader, A.; Pabel, M.; Willis, A. C.; Wild, S. B. First Resolution of a Free Secondary Phosphine Chiral at Phosphorus and Stereospecific Formation and Structural Characterization of a Homochiral Secondary Phosphine-Borane Complex. *Inorg. Chem.* **1996**, *35*, 3874-3877. (c) Albert, J.; Magali Cadena, J.; Granell, J.; Muller, G.; Panyella, D.; Sañudo, C. Resolution of Secondary Phosphanes Chiral at Phosphorus by Means of Palladium Metallacycles. *Eur. J. Inorg. Chem.* **2000**, 1183-1186.

22. (a) Huang, Y.; Li, Y.; Leung, P.-H.; Hayashi, T. Asymmetric Synthesis of P-Stereogenic Diarylphosphinites by Palladium-Catalyzed Enantioselective Addition of Diarylphosphines to Benzoquinones. *J. Am. Chem. Soc.* **2014**, *136*, 4865–4868. (b) Muldoon, J. A.; Varga, B. R.; Deegan, M. M.; Chapp, T. W.; Eördögh, Á. M.; Hughes, R. P.; Glueck, D. S.; Moore, C. E.; Rheingold, A. L. Inversion of Configuration at the Phosphorus Nucleophile in Diastereoselective and Enantioselective Synthesis of P-Stereogenic *syn*-Phosphiranes from Chiral Epoxides. *Angew. Chem. Int. Ed.* **2018**, *57*, 5047–5051. (c) Wang, C.; Huang, K.; Ye, J.; Duan, W.-L. Asymmetric Synthesis of P-Stereogenic Secondary Phosphine-Boranes by an Unsymmetric Bisphosphine Pincer-Nickel Complex. *J. Am. Chem. Soc.* **2021**, *143*, 5685–5690.

23. (a) Gibbons, S. K.; Valleau, C. R. D.; Peltier, J. L.; Cain, M. F.; Hughes, R. P.; Glueck, D. S.; Golen, J. A.; Rheingold, A. L. Diastereoselective Coordination of P-Stereogenic Secondary Phosphines in Copper(I) Chiral Bis(phosphine) Complexes: Structure, Dynamics, and Generation of Phosphido Complexes. *Inorg. Chem.* **2019**, *58*, 8854-8865. (b) Wang, G.; Gibbons, S. K.; Glueck, D. S.; Sibbald, C.; Fleming, J. T.; Higham, L. J.; Rheingold, A. L. Copper–Phosphido Intermediates in Cu(IPr)-Catalyzed Synthesis of 1-Phosphapyracenes via Tandem Alkylation/Arylation of Primary Phosphines. *Organometallics* **2018**, *37*, 1760–1772. (c) Gibbons, S. K.; Xu, Z.; Hughes, R. P.; Glueck, D. S.; Rheingold, A. L. Chiral Bis(Phospholane) PCP Pincer Complexes: Synthesis, Structure, and Nickel-Catalyzed Asymmetric Phosphine Alkylation. *Organometallics* **2018**, *37*, 2159–2166. (e) Glueck, D. S. Catalytic Asymmetric Synthesis of P-Stereogenic Phosphines: Beyond Precious Metals. *Synlett* **2021**, *32*, 875-884. (f) ref 15.

24. Langford, C. H.; Gray, H. B. *Ligand Substitution Processes*; W. A. Benjamin, New York, 1966.

25. (a) Rogers, J. R.; Wagner, T. P. S.; Marynick, D. S. Metal-Assisted Pyramidal Inversion in Metal-Phosphido Complexes. *Inorg. Chem.* **1994**, *33*, 3104-3110. (b) Geer, A. M.; Tejel, C. Organo-phosphanide and -phosphinidene complexes of Groups 8–11. *Adv. Organomet. Chem.* **2022**, *77*, 243-330.

26. Tipker, R. M.; Hughes, R. P.; Glueck, D. S.; Spinney, H. A.; Brammer, M. A.; Rheingold, A. L. Displacement of P-Stereogenic Phosphiranes from Rhodium by CO in Hydroformylation Catalysis. *Organometallics* **2024**, *43*, 427-431.

27. Glueck, D. S. Metal–Catalyzed P–C Bond Formation via P–H Oxidative Addition: Fundamentals and Recent Advances. *J. Org. Chem.* **2020**, *85*, 14276–14285.

28. Varela-Izquierdo, V.; Geer, A. M.; de Bruin, B.; López, J. A.; Ciriano, M. A.; Tejel, C. Rhodium Complexes in P−H Bond Activation Reactions. *Chem. – Eur. J.* **2019**, *25*, 15915-15928.

29. Gordon, B. M.; Lease, N.; Emge, T. J.; Hasanayn, F.; Goldman, A. S. Reactivity of Iridium Complexes of a Triphosphorus-Pincer Ligand Based on a Secondary Phosphine. Catalytic Alkane Dehydrogenation and the Origin of Extremely High Activity. *J. Am. Chem. Soc.* **2022**, *144*, 4133-4146.

30. Malakar, S.; Gordon, B. M.; Mandal, S.; Emge, T. J.; Goldman, A. S. Ruthenium Complexes of a Triphosphorus-Coordinating Pincer Ligand: Ru-P Ligand-Substituent Exchange Reactions Driven by Large Variations of Bond Energies. *Inorg. Chem.* **2023**, *62*, 4525-4532.

31. Seeman, J. R. Effect of Conformational Change on Reactivity in Organic Chemistry. Evaluations, Applications, and Extensions of Curtin-Hammett/Winstein-Holness Kinetics. *Chem. Rev.* **1983**, *83*, 83-134.

32. Knizia, G. Intrinsic Atomic Orbitals: An Unbiased Bridge between Quantum Theory and Chemical Concepts. *J. Chem. Theory Comput.* **2013**, *9*, 4834-4843.

33. (a) Knizia, G.; Klein, J. E. M. N. Electron Flow in Reaction Mechanisms—Revealed from First Principles. *Angew. Chem. Int. Ed.* **2015**, *54*, 5518-5522. (b) Tsuneda, T.; Sumitomo, H.; Hasebe, M.; Tsutsumi, T.; Taketsugu, T. Reactive orbital energy theory serving a theoretical foundation for the electronic theory of organic chemistry. *J Comput. Chem.* **2023**, *44*, 93-104.

34. Han, L.-B.; Zhao, C.-Q.; Onozawa, S.; Goto, M.; Tanaka, M. Retention of Configuration on the Oxidative Addition of P-H Bond to Platinum (0) Complexes: The First Straightforward Synthesis of Enantiomerically Pure P-Chiral Alkenylphosphinates via Palladium-Catalyzed Stereospecific Hydrophosphinylation of Alkynes. *J. Am. Chem. Soc.* **2002**, *124*, 3842-3843.

35. (a) Moncarz, J. R.; Brunker, T. J.; Glueck, D. S.; Sommer, R. D.; Rheingold, A. L. Stereochemistry of Palladium-Mediated Synthesis of PAMP-BH_3: Retention of Configuration at P in Formation of Pd-P and P-C Bonds. *J. Am. Chem. Soc.* **2003**, *125*, 1180-1181. (b) Moncarz, J. R.; Brunker, T. J.; Jewett, J. C.; Orchowski, M.; Glueck, D. S.; Sommer, R. D.; Lam, K.-C.; Incarvito, C. D.; Concolino, T. E.; Ceccarelli, C.; Zakharov, L. N.; Rheingold, A. L. Palladium-Catalyzed Asymmetric Phosphination. Enantioselective Synthesis of PAMP-BH_3, Ligand Effects on Catalysis, and Direct Observation of the Stereochemistry of Transmetalation and Reductive Elimination. *Organometallics* **2003**, *22*, 3205-3221.

36. Cain, M. F.; Hughes, R. P.; Glueck, D. S.; Golen, J. A.; Moore, C. E.; Rheingold, A. L. Synthesis and Structure of Intermediates in Copper-Catalyzed Alkylation of Diphenylphosphine. *Inorg. Chem.* **2010**, *49*, 7650–7662.

37. Pangborn, A. B.; Giardello, M. A.; Grubbs, R. H.; Rosen, R. K.; Timmers, F. J. Safe and Convenient Procedure for Solvent Purification. *Organometallics* **1996**, *15*, 1518-1520.

38. Scheetz, P. M.; Blank, N. F.; Gibbons, S. K.; Glueck, D. S.; Rheingold, A. L. Oxidative Addition of Methylene Chloride to Me-DuPhos Complexes of Palladium and Rhodium. *Inorg. Chim. Acta* **2018**, *483*, 111-115.

39. Friedfeld, M. R.; Shevlin, M.; Hoyt, J. M.; Krska, S. W.; Tudge, M. T.; Chirik, P. J. Cobalt Precursors for High-Throughput Discovery of Base Metal Asymmetric Alkene Hydrogenation Catalysts. *Science* **2013**, *342*, 1076-1080.

40. Cowley, A. H.; Norman, N. C.; Pakulski, M. Phosphorus Compounds Containing Sterically Demanding Groups. *Inorg. Synth.* **1990**, *27*, 235-240.

41. Brauer, D. J.; Bitterer, F.; Dorrenbach, F.; Hessler, G.; Stelzer, O.; Kruger, C.; Lutz, F. Synthesis, Coordination Chemistry and Ligand Properties of Secondary Phosphines R(Ar*)PH with Bulky Aromatic Substituents -- Molecular Structure of Ph(Is)PH, Is_2PH and ClAu[PhPMes*H]. *Z. Naturforsch. B* **1996**, *51*, 1183-1196.

Table of Contents Graphic